Interplay between crystal-field splitting and superexchange interaction in the t_{2g} orbital Mott insulator

Sergey Krivenko*

Institute of Physics, Kazan Federal University, Kremlyovskaya Street 18, 420008 Kazan, Russia

(Received 7 July 2011; revised manuscript received 10 January 2012; published 14 February 2012)

With a model of the $d^1(t_{2g})$-electron antiferromagnetic Mott insulator a competition of two typical interactions for orbital states of the t_{2g}-triplet levels has been investigated: The on-site electronic coupling with a local crystal field (LCF) tends orbitals to order, while the intersite superexchange (SE) induces their fluctuations. Both interactions coexist in perovskites: The LCF is induced by $GdFeO_3$-type structural deformations. In turn, the SE originates from virtual electronic hoppings, allowed by the Pauli principle, between nonorthogonal orbital states of adjacent sites. The dependence of the state of the orbitals (namely, a dispersion of their excitations and the quadrupole polarization) on a relation between the energy Δ of the triplet level splitting, caused by the D_{3d}-symmetry LCF, and the exchange energy $J_{\rm SE}$ is analyzed. Two qualitatively different regimes of the collective orbital behavior have been established: the induced order and fast fluctuations. It has been found that a crossover between them occurs when Δ comes close to $J_{\rm SE}$, and in the parameter region about $\Delta \approx J_{\rm SE}$ the order and fluctuations affect the wave function in a comparable extent. Previous approaches based on either of the interactions fail in this window. The present study identifies validity ranges of the former theories, embracing the physics of the orbitals by the unified description.

DOI: 10.1103/PhysRevB.85.064406 PACS number(s): 75.25.Dk, 71.70.−d, 75.30.Et, 75.30.−m

I. INTRODUCTION

Orbital quantum numbers of strongly correlated electrons, residing in the $3d(4d)$ shell of transition metal (TM) ions, are important control parameters for complex properties of TM oxides: their intricate ground states, low-energy excitations, and phase transitions.[1] A realization that the d-orbital variables should be considered on the same foundations with spin ones in these materials has stimulated an establishment of a modern branch of science: orbital physics.[2] The canonical but still challenging subjects of the research are the Mott insulators with a simple perovskite pseudocubic lattice RBO_3 [R^{3+} and B^{3+} correspond to a rare-earth (RE) and TM ions, respectively], where the d electrons are localized by the strong Coulomb on-site repulsion while their spin and orbital degrees of freedom survive.[1–6] Keeping an energy degeneracy of the ionic d eigenstates in part, a ligand crystal field of idealized cubically symmetric oxygen octahedrons retains for the orbital system some freedom to chose their ground state. The field splits the d level into a doublet of the e_g wave functions (x^2-y^2, $3z^2-r^2$) directed along the bonds B-O and a triplet of the t_{2g} orbitals (xy, xz, yz) lying in the octahedron basal planes. A consequent problem of the degeneracy resolving belongs to basic issues of orbital theory, stimulating investigations of mechanisms selecting a peculiar state from many of such in the system.

Typical relevant interactions of the d electrons in the perovskites are their intersite superexchange (SE) and the electric coupling with a local crystal field (LCF) at a TM site, which is introduced by a deformation of the oxide structure.[3–6] In a case of the ions with the active e_g orbitals (B = Mn, Cu, etc.), both interactions create a long-range orbital order, promoting each other.[4,7] Originally, for the systems with the t_{2g} symmetry (B = Ti, V) the similar picture of a cooperation between the SE and the LCF orbital orders was suggested.[8,9] However, refined analyses have revealed that models, engaging only *one* of these orbital interactions—either SE (*I*), or LCF (*II*)—predict fundamentally different behavior of the t_{2g} orbitals: In the first case, strong vacuum fluctuations stabilize either quantum disorders [e.g., the orbital liquid[10–14] (OL) and orbital Peierls state[15,16]] or quantum orders;[17,18] while captured by the static distortions, the d orbitals form classical orders[19–22] in the second case.

In last decade the former[6,10–18] (*I*) and the latter[5,19–32] (*II*) approaches (sometime called schemes[32]) have been developed into actual directions of research, reaching remarkable success in quantitative descriptions of the experimental properties of t_{2g} oxide materials (titanates,[33–40] vanadates[41–43]) from the opposing principles (cf., for instance, Refs. 10–12 with Refs. 19–26). A controversy emerged as to which of them is more appropriate.[5,6] *De facto*, the SE and LCF interactions are present in perovskites together,[5,6] but their coexistence and concurrence for the t_{2g} orbital state were not modeled; as a consequence, it has not been determined when each of these schemes collapses. The existence of the theoretical "gap" between these conflicting doctrines hinders an entire comprehension of the t_{2g} orbital physics.

The present work is a first attempt to obtain a generalized model, based on *both* competing interactions, which could reconcile conflicting scenarios (*I*) and (*II*) of the t_{2g} orbital states, embracing the approaches by a unifying description and separating them into distinct parametric validity regimes. To this end, I have investigated how the orbital system organization adopts the alternative tendencies due to the competition between the SE and LCF for the t_{2g} state. Also, the universal approach could reflect a bifacial character of the t_{2g} orbitals, appearing in the numerous low-temperature experiments: One set of them detected the robust orbital order,[21,35,36,41] while the other set indicated the powerful quantum fluctuations.[37–40,42,43] I have chosen the $d^1(t_{2g})$-electronic Mott insulator with the cubic TM sublattice and G-type antiferromagnetic (AFM) spin arrangement as a representative variant of the problem.

The impressive distinction between the predictions, given by the "pure"-SE (*I*) and LCF (*II*) interaction scheme,

for the t_{2g} orbital behavior [respectively the quantum OL phase[10–12] and static induced orbital order (IOO) "dictated" by a distortion[19–22]], becomes apparent in the research of the puzzling spin G-type AFM Mott insulator $LaTiO_3$. A motivation of those numerous studies was to find an orbital ground state of the $d^1(t_{2g})$ electrons of Ti^{3+} ions, which is capable of reconciling the spatial anisotropy of the t_{2g} orbitals underlying the SE with the cubic symmetry of the magnetic spectrum[33] and absence of a cooperative Jahn-Teller (JT) transition in the lattice.[34] Below, we outline concisely corresponding approaches (*I*) and (*II*).

The first of them (the pure-SE model of the OL) has been suggested in Ref. 10. The OL is a collective resonance of the spin/orbital excitations of valence bonds between the d^1 ions in the cubic lattice, which minimizes the energy of the AFM state through a dynamical lifting of the t_{2g}-triplet degeneracy with the maintenance of the spacial symmetry group.[10–12] In the Mott insulator with the quasilocalized d electrons the SE interaction between their spins establishes in a bond connecting nearest sites. The physical process is a virtual electron hopping across the charge gap allowed by the Pauli principle and retaining partially the kinetic energy.[44] The hopping parameters strongly depend on the orbital structure, and in the case of the degenerate e_g or t_{2g} levels the spin and orbital variables enter the SE models on equal footing and become mutually coupled.[3,45] The intersite exchange by these quantum numbers introduces fluctuations.

The energy of the SE spin/orbital correlations/fluctuations could be optimized in diverse fashions, depending on the symmetry of the active orbitals.[3,4,6] A nonequivalence of the SE interaction for the wave functions of the e_g doublet is responsible for the spontaneous long-range orbital order.[3,4] On the contrary, in the t_{2g} system an SE bond involves a doublet of the equivalent planar orbitals.[6,10] The quantum resonance between such degenerate configurations produces cooperative states with the fast on-site orbital fluctuations, lifting off the triplet degeneracy completely. When all the three t_{2g} orbitals could be operable like for the d^1 (Ti^{3+}) ion, the AFM OL is formed. It is composed of the dynamic bonds evenly intermixed over the cubic lattice, which entangle spin and orbital variables.[10,12,14] If only a pair of the orbitals remains SE active in this way, as for the d^2 (V^{3+}) ion, the orbital-only intersite singlets in the spontaneously dimerized bonds become favorable.[16]

According to scenario (*I*), it is just these orbital oscillations, developed close to the Mott transition, that obstruct the JT orbital-lattice order in lanthanum titanate.[10] The recent Raman[38] and RIXS[39] (resonant inelastic x-ray scattering) measurements corroborate the picture of the fast collective t_{2g} orbital fluctuations.

In the alternative framework,[19–32] the LCF caused by the lattice distortions controls the orbitals at a TM site instead of the SE. For the states with the t_{2g} symmetry the interaction with the $GdFeO_3$-type intrinsic perovskite deformation (GFOD), trigged by ionic size mismatch effects, is crucial.[19]

In the GFOD structure a variation of the R-ionic radius becomes accommodated by cooperative tilts and rotations of the oxygen octahedra to adjust the energy of the R-O bonds, the smaller ion affects the crystal more. With the shape of the octahedra and d-element cubic sublattice remaining relatively firm, the TM and RE ions were found to be shifted against each other pronouncedly.[5] Namely, in $LaTiO_3$ one of the body Ti-La diagonals is shorter, suggesting the lowest t_{2g}-electronic crystal-field state exhibiting the character of the e_g wave function extended toward the R cation.[19–22] Such a state is in agreement with the x-ray[21] and NMR[35] (nuclear magnetic resonance) experiments. Having lifted the degeneracy of the t_{2g} orbitals "disposed" toward it, the GFOD prohibits the JT effect from carrying this out by means of the spontaneous squeezing of the octahedra to lower the electron-lattice energy.[19,20] Actually, for the t_{2g} electrons the JT mechanism is less efficient than the GFOD, because lobes of such orbitals are directed apart from the anionic site.

Analysis in Refs. 19 and 20 has shown that the shift of the RE La ions generates the LCF on the TM sites with the symmetry close to the D_{3d} trigonal distortion.[30] The LCF splits the t_{2g} triplet and statically orders the orbitals in the ground nondegenerate a_{1g} level screened by the energy gap Δ against *local* doublet excitations e'_g. The trigonal symmetry of the a_{1g} states of the d^1 electrons implies the uniform AFM SE coupling between their spin $= 1/2$ for all the bonds[30] in correspondence with the cubic symmetry of the experimental magnon spectrum.[33] Unlike approach (*I*) the low-energy physics is expressed by the pure-spin SE models[19,20,23–25] in scheme (*II*).

The closeness of estimated realistic magnitudes of these basic orbital interactions, the SE and LCF ones,[46] is an additional, practical reason in favor of the consideration of their interplay within the unifying theoretical approach.

In the present work I have analyzed how the competition between the SE and LCF for the t_{2g} orbital degrees of freedom of the d^1 electrons in their AFM spin state could be resolved at zero temperature. The effective model, incorporating the coupling of the t_{2g} orbitals to the on-site GFOD-LCF with the D_{3d} symmetry and the intersite spin-orbital SE interaction in the cubic lattice as well, has been introduced in Sec. II. The orbital state has been investigated in a dependence on the respective scales, Δ and J_{SE}, of these contributions in the Hamiltonian, which served as parameters. Increasing of Δ/J_{SE} corresponds to enhancing GFOD in the AFM titanates from the domain of compositions with the relatively large-radius RE ions (La, Ce, Pr) upon their partial or complete substitution by the more compact ones (say La to Ce or Pr): In this trend the amplification of the local trigonal crystal field at a TM site due to shifts of the RE cations goes hand in hand with an attenuation of the intersite SE constant for the t_{2g} orbitals caused by the canting of the Ti-O-Ti bond.[5,19,20]

Taking the static IOO with the localized orbital states as an initial approximation, I have revealed a development of the nonlocal fluctuations due to the spin-orbital SE, treated as a perturbation. In Sec. III an analytical description of the collective orbital dynamics has been obtained. In Sec. IV two different regimes of the extended quantum fluctuations have been established: one with the IOO-likeness and another with OL-likeness. A parametric condition segregating them has been deduced. In Sec. V a parameter of the orbital order has been calculated, indicating a crossover between the IOO and OL. A general discussion is presented in Sec. VI.

II. ORBITAL MODEL

A. Superexchange interaction

Following the Kugel-Khomskii (KK) approach for low-energy states of a perovskite Mott insulator with the orbital degrees of freedom,[3,45] I start from a hypothetical cubic lattice, corresponding to TM ions, where each site i possesses only one $d(t_{2g})$ electron. Then in the bond $\langle ij\rangle$ the electronic SE interaction arises from the virtual transitions to the upper Hubbard band $d_i d_j \leftrightarrow d^2_{i(j)}$ with the amplitude t, while the low-energy charge excitations are quenched by the strong on-site Coulomb repulsion U, being the dominant energy in the issue. For the sake of simplicity, the SE bonds are considered here in the limit of vanishing on-site Hund exchange interaction, because usually its relative strength is small: $J_{\rm H}/U \ll 1$.

In the case of the triple degenerate local t_{2g} levels the SE is described by the spin-orbital KK model,[45] which could be reduced to the form[11,12,18]

$$H_{\rm SE} = J_{\rm SE}\sum_{\langle ij\rangle_\gamma} A_{ij}^{(\gamma)}\left(\vec{S}_i\vec{S}_j + \frac{1}{4}\right). \qquad (1)$$

Here the parameter $J_{\rm SE}$ $(= \frac{4t^2}{U} > 0)$ sets the energy scale of the SE interaction. The operators $\vec{S}$ stand for the electronic spins $S = 1/2$, and their orbital-dependent intersite coupling are determined by the operators $A_{ij}^{(\gamma)}$, acting in the basis of the cubic harmonics yz, xz, xy (each of them is denoted by the respective direction a, b, c of the bond γ orthogonal to its plane). Namely, for the lattice bond c the orbital operator can be written as

$$A_{ij}^{(c)} = n_{i,a}n_{j,a} + n_{i,b}n_{j,b} + a_i^\dagger b_i b_j^\dagger a_j + b_i^\dagger a_i a_j^\dagger b_j, \qquad (2)$$

while the expressions for the other two bonds are obtained from (2) after cyclic permutations of the indexes a, b, and c. Also, in Eq. (2) the respective t_{2g} orbital states are represented by the spinless pseudoparticles (orbitons) a_i, b_i, c_i with the constraints $n_{i,a} + n_{i,b} + n_{i,c} = 1$ for their numbers.

The spin and orbital physics of the t_{2g}-KK model is highly nontrivial. Its internal symmetry favors strong fluctuations, preventing spin ordering at any nonzero temperature in the cubic lattice[47] by analogy with conventional planar spin systems.[48]

At $T = 0$ the exact ground state of Hamiltonian (1) is unknown, though it could be approached employing different approximations.[9,10,12,17,18] When the degrees of freedom in the SE interaction are decoupled into the spin and orbital sectors, the mean-field analysis in Ref. 9 indicates the KK model to be close to the quantum critical point between the ferromagnetic (FM) and AFM spin orderings, and the subsequent separate treatment of the spin/orbital vacuum fluctuations stabilizes the FM arrangement.[17,18] However, if the correlated, strongly coupled spin-orbital fluctuations are taken into account within the model of the OL,[10–12] the antiferromagnetism wins, bringing the better estimation of the SE energy.[10,18]

In fact, the staggered spin order is facilitated by the infinite orbital degeneracy (frustration) of the Néel phase of Hamiltonian (1) in the classical limit $\vec{S}_i\vec{S}_j = -1/4$, when the orbitals on each site could be rotated independently without energy costs.[10] The "order-from-disorder" mechanism[49] removes this degeneracy completely, selecting the AFM OL state with the help of the specific SE quantum fluctuations being very efficient due to the flat "geometry" of the t_{2g} orbitals.

To follow the way that the frustration becomes resolved it is instructive to compare the t_{2g} with e_g system. In the last case the regular e_g orbital order, forming the directional chainlike structure, maximizes the SE energy gain from the AFM spin fluctuations.[50,51] The t_{2g} orbitals are, however, not bond-directed, but planar. As a result, not much fluctuation energy in the AFM can be gained by any pattern of static t_{2g} orbital ordering, while their dynamic disordering turns out to be the advantageous solution.[10]

In the t_{2g} system the spin "exchange integral" $J_{\rm SE}A_{ij}^{(\gamma)}$ is confined to an individual pair of the equivalent orbitals for every SE bond [say only the a and b states are active for the bond c in Eq. (2)], thus having the extra SU(2) symmetry in the orbital subspace.[10,52] As is known from the spin SU(2) × orbital SU(2) models,[52–56] the main contribution to the exchange energy is gained in that case due to the resonance between degenerate local configurations (spin singlet × orbital triplet and spin triplet × orbital singlet), and the elementary excitations become collective composite modes with spin and orbital variables unified by the SU(4) symmetry. In particular, the ground state of the lattice turns out to be the nondegenerate SU(4)-isotropic one (singlet),[52,53] comprising every possible configuration of such four-site singlets[52,56] in a fashion of the Anderson's RVB (resonating valence bonds) wave functions.[57] Acquiring the best possible exchange energy per bond, these local spin-orbital singlets become perfect "building blocks" for the vacuum state.[52]

It was shown in Refs. 10 and 12 that even though a true SU(4) singlets cannot develop in model (1) because of its spin-orbital asymmetry, they provide for the t_{2g} system a way to resolve the frustration, minimizing the exchange energy by formation of the virtual SU(4) resonances composed of short-length spin fluctuations accompanied by instant dynamical orbital bonds. Since the singlets entangle spin and orbital degrees of freedom, a separate analysis of these variables is destructive for the resonances.[13,14] The OL, being the quantum phase of the rapidly oscillating orbitals with a gapless fermionic spectrum in the mean-field description (so-called $\chi - J$ model),[10] amplifies this mechanism in three dimensions of the lattice. Because the OL possesses the invariance against the cubic space group, the fluctuation-averaged exchange integrals become equivalent for all the bonds and facilitate the G-AFM order due to spontaneous breaking of the spin SU(2) symmetry[10,11] of SE interaction (1).

Apparently, the GFOD should inhibit the resonances, affecting the t_{2g} orbital degeneracy of the SE bonds. However, the theory of the OL, coexisting with distortions, is lacking, and there is no information about the magnitude of the LCF, which suppress the OL completely.

B. Local crystal field

Now we return to scheme (*II*), where the state of the orbital is determined by its coupling with the LCF, applied to the $d^1(t_{2g})$ electron due to the GFOD. For simplicity, we consider the equivalent LCF with the D_{3d} symmetry at every site i of

the cubic lattice; such periodicity corresponds to the uniform "configuration 1" in Ref. 30. The trigonal symmetry splits the cubic t_{2g} triplet into the singlet ground state with the wave function $a_{1g} = 3z^2_{[111]} - r^2$ extended along the direction [111] and the doublet e'_g of the gapped excitations. These orbitals are represented with the orbitons $\psi_{1,i}$, $\psi_{2,i}$, $\psi_{3,i}$ as follows:

$$a_{1g} : \psi_{1,i} = \frac{1}{\sqrt{3}}(a_i + b_i + c_i);$$
$$e'_g : \begin{cases} \psi_{2,i} = \frac{1}{\sqrt{2}}(a_i - b_i), \\ \psi_{3,i} = \frac{1}{\sqrt{6}}(2c_i - a_i - b_i). \end{cases} \tag{3}$$

The pseudoparticles, defined by Eqs. (3), satisfy the local constraints on their numbers: $n_{1,i} + n_{2,i} + n_{3,i} = 1$.

The corresponding Hamiltonian of the interaction between the orbitals and LCF is given by

$$H_{\rm LCF} = -\Delta \sum_i \frac{2n_{1,i} - n_{2,i} - n_{3,i}}{3}, \tag{4}$$

where the parameter $\Delta > 0$ denotes the energy of the trigonal crystal-field-induced gap. A condensation of the orbitons in the ground level $a_{1g} \equiv \psi^\dagger_{1,i}|0\rangle$ in each site produces the uniform static IOO due to the bosonic statistics, employed for fields (3) here. Again, the intersite SE interaction between the electrons, occupying the nondegenerate a_{1g} orbitals, creates the G-AFM spin order.[19,30]

Treating the ordered orbital and spin variables separately in the above fashion, the LCF approach effectively decouples them.[20] For this reason, in the present work we study the SE *coupling* between this sectors to clarify the nature of the t_{2g} orbital state. Also, such analysis lets us establish the condition, when the orbital order becomes unstable against the quantum fluctuations introduced by the SE, and approximation (*II*) fails.

Hereafter, the overcondensate excitations $\psi^\dagger_{2(3),i}$ are described with a compact form of interaction (4), where the fields $\psi_{1,i}$ are eliminated due to the constraints. The diagonality of operator (4) with respect to index i accounts for the local character of the orbital excitations pinned to their sites in the LCF scheme.

C. Interplay between the superexchange and crystal-field interactions of the orbitals

To investigate the competition of LCF and SE interactions for the t_{2g} orbital state upon varying a relation between the magnitudes of Δ and $J_{\rm SE}$, I consider the model

$$H = H_{\rm LCF} + H_{\rm SE} \tag{5}$$

at zero temperature. Here, $H_{\rm LCF}$ and $H_{\rm SE}$ are given by Eqs. (4) and (1), respectively.

Qualitatively, the first contribution to Eq. (5) facilitates the IOO state of the $d^1(t_{2g})$ electrons with the spin AFM arrangement, whereas the second term promotes the dynamical OL-like orbital disordering. Hence, the behavior of the t_{2g} orbital system in the antiferromagnet could be followed from the evolution of the orbital order.[58] To find it, for Hamiltonian (5) the classical IOO due to the LCF with local orbital excitations, described by operator (4), is taken as an initial approximation. Then the spin-orbital interaction $H_{\rm SE}$ is interpreted as a perturbation, because the spin factor in Eq. (1) becomes small in the Néel phase: For instance, in the aforesaid classical limit for the antiferromagnet it vanishes, and in the linear spin-wave theory $\langle \vec{S}_i \vec{S}_j + \frac{1}{4}\rangle \approx -0.05$. Consequently, such analysis is justified not only at $J_{\rm SE}/\Delta \ll 1$ but could be extended even up to the experimentally related situation[46] $J_{\rm SE} \approx \Delta$.

To investigate quantitatively the effect of the quantum spin-orbital oscillations, introduced by the SE, the mean fields and fluctuations about it are defined as follows:

$$A^{(\gamma)}_{ij} = \langle A^{(\gamma)}_{ij}\rangle + \delta A^{(\gamma)}_{ij}, \tag{6}$$
$$\vec{S}_i \vec{S}_j + \tfrac{1}{4} = \langle \vec{S}_i \vec{S}_j + \tfrac{1}{4}\rangle + \delta(\vec{S}_i \vec{S}_j) \approx \delta(\vec{S}_i \vec{S}_j). \tag{7}$$

According to this, SE operator (1) is separated into three contributions:

$$H_{\rm SE} = H_{\rm sp} + H_{\rm orb} + H_{\rm int}. \tag{8}$$

With the first two terms $(H_{\rm sp} + H_{\rm orb})$ in Eq. (8) the antiferromagnet, orbitally ordered by the LCF, is treated in the Hartree-Fock approximation, when the spin and orbital variables are decoupled. Namely, the intersite AFM spin interaction is described by the first contribution,

$$H_{\rm sp} = J_{\rm SE} \sum_{\langle ij\rangle_\gamma} \langle A^{(\gamma)}_{ij}\rangle \left(\vec{S}_i \vec{S}_j + \frac{1}{4}\right), \tag{9}$$

and the orbital correction is presented by the second one,

$$H_{\rm orb} = J_{\rm SE} \sum_{\langle ij\rangle_\gamma} \left\langle \vec{S}_i \vec{S}_j + \frac{1}{4}\right\rangle \delta A^{(\gamma)}_{ij} \approx 0. \tag{10}$$

From here on we omit term (10), being unessential in the AFM-IOO phase because of the aforementioned smallness of the spin correlator. The last contribution in Eq. (8) introduces the coupling between the correlated spin and orbital fluctuations about the Hartree-Fock states in the antiferromagnet:

$$H_{\rm int} = J_{\rm SE} \sum_{\langle ij\rangle_\gamma} \delta(\vec{S}_i \vec{S}_j) \delta A^{(\gamma)}_{ij}. \tag{11}$$

Our goal is to establish how interaction (11), treated as a perturbation in model (5), gaining the form

$$H = H_{\rm LCF} + H_{\rm sp} + H_{\rm int}, \tag{12}$$

affects the orbital sector, and when the IOO (generated by $H_{\rm LCF}$ in the antiferromagnet represented by $H_{\rm sp}$) becomes defeated due to the term $H_{\rm int}$ in Eq. (12).

Toward this end in view we implement expansion (6) of operator (2) with respect to the orbital fluctuations, being the virtual transitions from the ordered ground state a_{1g} to the doublet e'_g owing to spin-orbital coupling (11). This is achieved in three steps. (i) First, the fields a, b, c are represented through bosons (3). (ii) Then in the obtained expressions the variable ψ_1 is expanded in the series,

$$\psi_1 = \psi^\dagger_1 = \sqrt{1 - \psi^\dagger_2\psi_2 - \psi^\dagger_3\psi_3} \approx 1 - \tfrac{1}{2}(n_2 + n_3), \tag{13}$$

at each site i. Relation (13) is just the consequence of the local constraint for the orbitons and reflects an exhausting of their condensate due to the spontaneous $\psi^\dagger_{2(3),i}$ excitations. (iii) Having substituted the resultant expressions for a_i, b_i, c_i

into Eq. (2), required decoupling (6) of the orbital operator is realized as follows:

$$A_{ij}^{(\gamma)} = \tfrac{4}{9} + \delta A_{ij}^{(\gamma)}. \tag{14}$$

Here the first contribution corresponds to the expectation value,

$$\left\langle A_{ij}^{(\gamma)} \right\rangle = 4/9, \tag{15}$$

in the state with the perfect IOO, when all the orbitals occupy the a_{1g} level. Equation (15) provides the first-order estimation of the AFM spin interaction strength $J \equiv J_{\rm SE}\langle A_{ij}^{(\gamma)}\rangle = 4J_{\rm SE}/9$ in (9). Again, in Eq. (14) the fluctuation part reads as

$$\delta A_{ij}^{(\gamma)} = A_{ij}^{(\gamma)}(1) + A_{ij}^{(\gamma)}(2), \tag{16}$$

where the contributions of the first order $[A_{ij}^{(\gamma)}(1)]$ and second order $[A_{ij}^{(\gamma)}(2)]$ with respect to the orbital excitations are taken into account. Namely,

$$A_{ij}^{(\gamma)}(1) = \sum_{m=2}^{3} \alpha_m^{(\gamma)} (\psi_{m,i}^{\dagger} + \psi_{m,j}^{\dagger}) + \text{H.c.}, \tag{17}$$

with the coefficients $\alpha_2^{(a)} = -\alpha_2^{(b)} = -\sqrt{6}/9$, $\alpha_2^{(c)} = 0$, $\alpha_3^{(a)} = \alpha_3^{(b)} = -\alpha_3^{(c)}/2 = \sqrt{2}/9$. The lengthy expression for the term $A_{ij}^{(\gamma)}(2)$ is presented in Appendix A.

In accordance with Eq. (16) spin-orbital interaction (11) is expanded into the one- and two-orbiton parts $H_{\rm int}(1)$ and $H_{\rm int}(2)$, corresponding to the linear $A_{ij}^{(\gamma)}(1)$ and quadratic $A_{ij}^{(\gamma)}(2)$ orbital operators:

$$H_{\rm int} = H_{\rm int}(1) + H_{\rm int}(2). \tag{18}$$

Here we retain only the lowest order contribution $H_{\rm int}(1)$ in the interaction $H_{\rm int}$. Then term (11) in Hamiltonian (12) is reduced to the factored three-particle operator:

$$H_{\rm int} = \frac{J_{\rm SE}}{2} \sum_{\langle ij \rangle_\gamma} \left(s_i s_j + s_i^{\dagger} s_j^{\dagger} + n_i^s + n_j^s \right) \times \sum_{m=2}^{3} \left[\alpha_m^{(\gamma)} (\psi_{m,i}^{\dagger} + \psi_{m,j}^{\dagger}) + \text{H.c.} \right], \tag{19}$$

where the spin-flip processes are represented by the Néel magnons $s_i^{\dagger}$ ($n_i^s = s_i^{\dagger} s_i$ describes their number). [$H_{\rm int}(2)$ is obtained in Appendix A. The effects of $H_{\rm int}(1)$ and $H_{\rm int}(2)$ on the orbital state are compared in Appendix B within a second-order perturbation theory, the role of $H_{\rm int}(2)$ being minor.[59]]

The spin-orbital interaction $H_{\rm int}$ "shakes" the IOO in the antiferromagnet, admixing the spontaneous orbital fluctuations $\psi_{2(3),i}^{\dagger}|0\rangle$ to the vacuum of the orbitons, condensed in the local a_{1g} levels. This becomes evident from Eq. (19), containing nonzero matrix elements for the corresponding transitions from the ground to the exited states. Namely, such orbital fluctuation on a site i appears simultaneously with the intersite spin fluctuations on its adjacent bonds (i,j). In turn, the exchange of the nearest sites i and j by magnons creates the orbital excitation on the opposite site j of the bond, thus promoting tunneling of the orbitons over the lattice. In this fashion SE coupling (11) transforms the local e_g'-orbital excitations in the IOO state to the extended ones, correlating them with the intersite spin flips.

III. ORBITAL GREEN'S FUNCTIONS

The SE-driven collective orbital dynamics is investigated with Hamiltonian (12), taken in the momentum representation. Three-particle interaction (19) leads to the system of Dyson equations for the orbitons, written as

$$\begin{cases} \hat{G}_{i\omega,\vec{k}} = G_{i\omega}^0 \hat{I} + G_{i\omega}^0 \hat{S}_{i\omega,\vec{k}} (\hat{G} + \hat{F})_{i\omega,\vec{k}}, \\ \hat{F}_{i\omega,\vec{k}} = G_{i\omega}^{0\,*} \hat{S}_{i\omega,\vec{k}} (\hat{G} + \hat{F})_{i\omega,\vec{k}}. \end{cases} \tag{20}$$

Here the following notations have been used: Fourier components of the normal and anomalous thermal Green's functions, defined on the set of Matsubara frequencies $i\omega$, are $G_{i\omega,\vec{k}}^{mn} = \langle -T_\tau \psi_{m,\vec{k},\tau} \psi_{n,\vec{k},0}^{\dagger} \rangle_{i\omega}$ and $F_{i\omega,\vec{k}}^{mn} = \langle -T_\tau \psi_{m,-\vec{k},\tau}^{\dagger} \psi_{n,\vec{k},0}^{\dagger} \rangle_{i\omega}$ (m and $n = 2$ or 3). They are given by 2×2 matrices $\hat{G}_{i\omega,\vec{k}}$ and $\hat{F}_{i\omega,\vec{k}}$ in the orbital subspace ($\hat{I}$ is the unit matrix). The zero-order Green's function, $G_{i\omega}^0 = 1/(i\omega - \Delta)$, represents the localized orbital excitation, while the self-energy matrix $\hat{S}_{i\omega,\vec{k}}$ describes the intersite orbiton tunneling via the spin flips in the SE bonds due to particle exchange processes (19).

The self-energy is calculated from skeleton diagram (a) in Fig. 1 in the lowest order. [The effect of correction (b) due to $H_{\rm int}(2)$ is evaluated in Appendix B being relatively small.] In the internal lines the magnon excitation energy, $\omega_{\vec{k}} = 3J(1 - \gamma_{\vec{k}}^2)^{1/2}$ with $\gamma_{\vec{k}} = (c_{k_x} + c_{k_y} + c_{k_z})/3$, is related to spin-term (9) of Hamiltonian (12).

As it is shown in Appendix C, matrix elements of the spin-orbital interaction $H_{\rm int}$, "coupling constants" (C5), vanish in the limit of small magnon momenta, thereby "decoupling" the extended orbitons and soft spin-modes from each other. Then in the diagram loop lines the dispersion of the "bare" magnons could be approximated by the Izing limit, $\omega_{\vec{k}} \to D = 3J_{\rm SE}\langle A_{ij}^{(\gamma)}\rangle$, since the main contribution to corresponding momentum summation (C4) over the Brillouin zone (BZ) comes from the short-wavelength spin excitations in the bonds.[60] After this, the present problem becomes trackable analytically: The components of the dynamical corrections, $\hat{S}_{i\omega,\vec{k}}$, are calculated as

$$S_{i\omega,\vec{k}}^{mn} = \frac{4DJ_{\rm SE}^2}{(i\omega)^2 - (2D)^2}\, c_{\vec{k}}^{mn}. \tag{21}$$

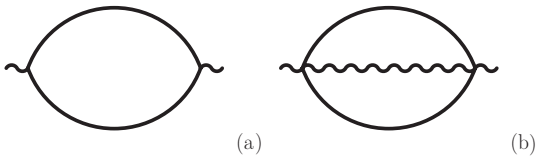

FIG. 1. Corrections (a) and (b) to the orbital excitations due to the contributions $H_{\rm int}(1)$ and $H_{\rm int}(2)$ in the spin-orbital interaction (18), respectively. Lines (wavy lines) correspond to the magnons (orbitons).

Here $\vec{k}$ dependencies are determined by the factors

$$c^{22}_{\vec{k}} = \frac{2}{27}(c_{k_x} + c_{k_y} + 2),$$
$$c^{23}_{\vec{k}} = c^{32}_{\vec{k}} = \frac{2}{27\sqrt{3}}(c_{k_y} - c_{k_x}), \tag{22}$$
$$c^{33}_{\vec{k}} = \frac{2}{81}(6 + c_{k_x} + c_{k_y} + 4c_{k_z}),$$

which arise in Eq. (21) due to the matrix elements of the interaction in the diagram vertices.

Then the orbiton functions, satisfying Eqs. (20), obtain the following structure:

$$G^{mn}_{i\omega,\vec{k}} = \frac{g^{mn}_{i\omega,\vec{k}}}{d_{i\omega,\vec{k}}}, \quad F^{mn}_{i\omega,\vec{k}} = \frac{f^{mn}_{i\omega,\vec{k}}}{d_{i\omega,\vec{k}}}, \tag{23}$$

where the numerators are defined by Eqs. (C7) (see Appendix C) and the denominator is given by

$$d_{i\omega,\vec{k}} = \prod_{l=1}^{2}\prod_{p=+,-}\left(i\omega - \omega^{p}_{l,\vec{k}}\right)\left(i\omega + \omega^{p}_{l,\vec{k}}\right). \tag{24}$$

Poles $\omega^{p}_{l,\vec{k}}$ of the causal Green's functions, obtained after the conventional analytic continuation of expressions (23) from the Matsubara frequencies, are indexed by $l = 1,2$, $p = +,-$ and correspond to four branches of the spectrum of the collective orbital excitations in the IOO state:

$$\omega^{\pm}_{l,\vec{k}} = \sqrt{\frac{\Delta^2 + 4D^2}{2}} \times \left\{1 \pm \left[1 - \frac{16\Delta D^2(\Delta - \Delta^*\alpha_{l,\vec{k}})}{(\Delta^2 + 4D^2)^2}\right]^{1/2}\right\}^{1/2}. \tag{25}$$

Here the momentum dependence is determined by functions

$$\alpha_{l,\vec{k}} = \frac{1}{2}\left[1 + \gamma_{\vec{k}} + (-1)^{l-1}\left(\frac{\kappa_{\vec{k}} - \gamma^2_{\vec{k}}}{2}\right)^{1/2}\right], \tag{26}$$

where $\kappa_{\vec{k}} = (c^2_{k_x} + c^2_{k_y} + c^2_{k_z})/3$. In Eq. (25) the prefactor of $\alpha_{l,\vec{k}}$ reads as follows:

$$\Delta^* = \frac{16}{27}\frac{J^2_{\rm SE}}{D} = \left(\frac{4}{9}\right)^2 J_{\rm SE}\left\langle A^{(\gamma)}_{ij}\right\rangle^{-1}. \tag{27}$$

Because $0 \leqslant \alpha_{l,\vec{k}} \leqslant 1$ [see Fig. 2(a)], energy (25) of the bosonic excitations possesses real, non-negative values in all the points $\vec{k}$ of the BZ only if the trigonal splitting

$$\Delta \geqslant \Delta^*. \tag{28}$$

In this case, the undamped orbiton modes appear in the IOO; the $\vec{k}$ dependence of their frequencies, $\omega^{p}_{l,\vec{k}}$, is presented in Figs. 2(b) and 2(c) upon decreasing Δ.

Dispersion (25) combined with expression (26) is invariant with respect to transformations of the cubic symmetry group in the reciprocal space. This acquired property of the orbital excitations in the local *trigonal* field is a "fingerprint" of the cubic symmetry of SE interaction (1) in their collective dynamics.

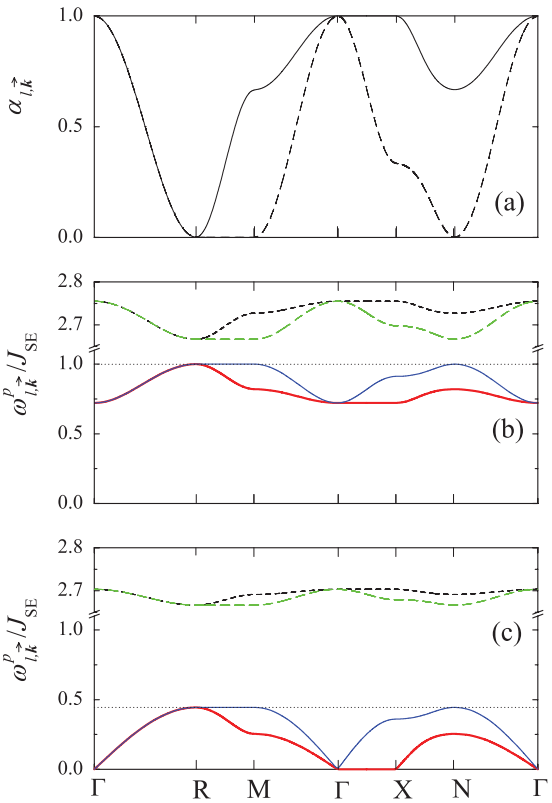

FIG. 2. (Color online) Momentum dependence of the orbital excitation spectrum along the path through the high-symmetry points $\Gamma = (0,0,0)$, $R = (\pi,\pi,\pi)$, $M = (\pi,\pi,0)$, $X = (\pi,0,0)$, and $N = (\pi,0,\pi)$. (a) Functions $\alpha_{l,\vec{k}}$ defined by Eq. (26): The solid (dashed) line corresponds to $l = 1$ (2). The orbiton dispersion, calculated from Eq. (25) with $\langle A^{(\gamma)}_{ij}\rangle = 4/9$, is plotted in panels (b) and (c) for the trigonal splitting $\Delta = J_{\rm SE}$ and $\Delta = \Delta^* = (4/9)J_{\rm SE}$, respectively; the energy of the corresponding local e'_g excitation is indicated by the horizontal dot lines. The lower branch $\omega^{-}_{1,\vec{k}}$ ($\omega^{-}_{2,\vec{k}}$) is drawn by the red (blue) solid line, and the upper one $\omega^{+}_{1,\vec{k}}$ ($\omega^{+}_{2,\vec{k}}$) is represented by the black (green) dashed line.

The spectral density of these excitations is evaluated in Appendix D from a normal Green's function (23) as follows: $\rho^{mn}_{p,l,\vec{k}}\,\delta(\omega - \omega^{p}_{l,\vec{k}})$. Here the factors $\rho^{mn}_{p,l,\vec{k}}$ are given by Eq. (D1a), being residues in the poles $\omega^{p}_{l,\vec{k}}$ [Eq. (25)]. The remaining poles, $-\omega^{p}_{l,\vec{k}}$ [see Eq. (24)] with the residues $\sigma^{mn}_{p,l,\vec{k}}$ [Eq. (D1b)], correspond to related vacuum zero-point orbital modes with frequencies (25) and spectral density $\sigma^{mn}_{p,l,\vec{k}}\,\delta(\omega + \omega^{p}_{l,\vec{k}})$. Such collective quantum oscillations of the ground state develop in the IOO due to the spontaneous e'_g excitations caused by spin-orbital interaction (19). Signs of a high-frequency cubic orbiton mode were detected in the Raman measurements in $R\mathrm{TiO_3}$.[38]

IV. ORBITAL EXCITATIONS

Here we analyze properties of the extended orbital excitations. When assumption (28) for the magnitude of the LCF holds, the subradical expression in the square brackets of Eq. (25) becomes non-negative. This implies the relation $\omega^{-}_{l,\vec{k}} \leqslant \omega^{+}_{l,\vec{k}}$ for the dispersion. Accordingly, the excitations are

split into two bundles of the branches: a "lower" $\omega^{-}_{l,\vec{k}}$ and an "upper" $\omega^{+}_{l,\vec{k}}$ one, as Figs. 2(b) and 2(c) illustrate. Keeping in mind that $\alpha_{1,\vec{k}} \geqslant \alpha_{2,\vec{k}}$ one obtains the following hierarchy of energies (25) of the orbital oscillations:

$$\omega^{-}_{1,\vec{k}} \leqslant \omega^{-}_{2,\vec{k}} \leqslant \omega^{+}_{2,\vec{k}} \leqslant \omega^{+}_{1,\vec{k}}. \tag{29}$$

The family $\omega^{-}_{l,\vec{k}}$ ($l = 1,2$) develops from the localized e'_g excitations over the initial crystal gap Δ, when they become deconfined from their sites owing to the virtual creation of magnon pairs in the neighboring SE bonds. The respective extended composite bosonic quasiparticles resemble propagating orbital excitations "dressed" by clouds of the magnons. They correspond to orbital waves in the IOO state. The residues of the poles $\omega^{-}_{l,\vec{k}}$ are pronounced: In specific directions of the reciprocal space the magnitudes $\rho^{mm}_{-,l,\vec{k}}$ are about unity (for a ratio $\Delta/J_{\rm SE} = 1$ close to the realistic one[46]), indicating the coherence of the modes [see panels (a), (b) in Fig. 4 in Appendix D]. The delocalization of these modified orbitons reduces their kinetic energy; as a result, the spectrum both sinks below the parent level Δ and obtains its dependence on the momentum [see Figs. 2(b) and 2(c)]. A moderate variation of the energy of the collective orbital excitations over the BZ indeed has been observed as in lanthanum and so in yttrium titanate in the recent RIXS experiments.[39]

When $\alpha_{l,\vec{k}} = 1$ the two branches $\omega^{-}_{l,\vec{k}}$ ($l = 1, 2$) simultaneously reach their minimum,

$$\omega_{\Delta} = 2D\sqrt{\frac{\Delta(\Delta - \Delta^{*})}{\Delta^{2} + 4D^{2}}}, \tag{30}$$

which is a renormalized gap for the orbital excitations. Gap (30), stabilizing the orbital order, promptly diminishes with Δ and collapses at $\Delta = \Delta^{*}$, indicating a lower bound of the IOO state: Further decreasing of Δ results in an imaginary value of ω_{Δ}. Then the lower energy branches $\omega^{-}_{l,\vec{k}}$ become complex functions, and consequently the wavelike orbital modes decay as a result of strong SE-driven fluctuations. Such a behavior points to an *instability* of the IOO and a different nature of the extended spin-orbital quasiparticles in the region $\Delta < \Delta^{*}$.

A peculiarity of function (26) with $l = 1$ is that it becomes $\alpha_{1,\vec{k}} = 1$ for every $\vec{k} = (k,0,0)$ [$(0,k,0)$ or $(0,0,k)$] in the interval $-\pi \leqslant k \leqslant \pi$. As a consequence, when $\Delta = \Delta^{*}$, gap (30) of the branch $\omega^{-}_{1,\vec{k}}$ simultaneously disappears along the three coordinate axes of the BZ (in the direction ΓX and equivalent ones) [see Fig. 2(c)]. The emergence of such lines of the soft excitations implies a fragility of the IOO state, because in the family of cubic planes (100) [(010) or (001)], which are orthogonal to the corresponding line, the orbitals obtain an ability to change their phase without energy costs independently of the others in neighboring parallel planes. As a result, the intensity of the quantum fluctuations of the ground state dramatically enhances: For the momenta, extended along these lines, the residues (D1) diverge as

$$\rho^{mm}_{-,1,\vec{k}} = -\sigma^{mm}_{-,1,\vec{k}} \sim \omega^{-1}_{\Delta}, \tag{31}$$

when Δ approaches Δ^{*}.[61] Such a trend is apparent in panels (c) and (d) of Figs. 4 and 5 in Appendix D.

An appearance of massless extended modes with a diverged spectral density of low-frequency vacuum fluctuations signifies an evolution of a system from its one regime to a qualitatively another. Such a behavior is typical, when a ground state rebuilds. As we see in the next section, this is accompanied by a suppression of a parameter of the orbital order.

The emergence of the aforesaid linear pieces of the gapless orbitons with an infinite degeneracy of states indicates that already at $\Delta \to \Delta^{*}$ one faces the problem of the orbital frustration, which was removed at $\Delta > \Delta^{*}$ in Hamiltonian (12) due to the applied trigonal crystal field splitting the triplets. As was obtained in Ref. 12 for pure-SE model (1) in the space of the degenerate triplets, interaction (11) leads to a strong coupling between the short-wavelength magnons and t_{2g} orbital fluctuations. Then a nonperturbative effect of such coupling results in the bound spin-orbital resonances, forming the OL phase.[12] For the present model, this analogy suggests that a continuum of low-lying OL-like excitations supersedes the soft fluctuational modes $\omega^{-}_{1,\vec{k}}$ in the orbital dynamics when Δ decreases below the scale Δ^{*}: The fast spin-orbital fluctuations lift the infinite orbital degeneracy of the vacuum, when gap (30) disappears.

Again, in the proximity of the critical scale Δ^{*}, when the IOO fails, the perturbational approach to model (12) becomes rather superficial. Nevertheless, it bears distinctive marks of the OL fermionic continuum in the dispersion of the extended excitations, such as the one-dimensional segments with the nonzero density of the (almost) gapless states.[10] Our estimation with spectrum (25) yields the reasonable density $\rho(0) = 0.11$ of the gapless modes when $\Delta \to \Delta^{*}$ (for $\langle A^{(\gamma)}_{ij} \rangle = 4/9$), which is about six times smaller than the density of states at the Fermi level in the genuine OL.[10] Such relative reduction of $\rho(0)$ correctly illustrates the tendency to suppress the low-lying SE-modes, when the gradually amplifying LCF is superimposed on the OL.

The instability of the ordered state of the t_{2g} orbitals, tending to the fluctuations due to the SE interaction, is a consequence of their peculiar planar geometry. This behavior is in contrast to the e_g system, where the SE coupling between the magnons and orbitons retains the gap and stabilizes the order in the orbital sector.[50]

Regarding the upper branches $\omega^{+}_{l,\vec{k}}$ ($l = 1, 2$) of dispersion (25), they always possess an open gap $2D$ [see Fig. 2(b) and 2(c)], which corresponds to the double energy of a spin-flip in the antiferromagnet. These "spinlike" poles of the Green's functions originate from a peculiar mixing of the orbital and spin variables, when the tunneling orbitons excite the AFM bonds and virtually "dissociate" into pairs of the magnons due to interaction (19). The spectral density factors $\rho^{mm}_{+,l,\vec{k}}$ for such orbitons are by some orders of magnitudes less than those for the lower branches. Thus, the orbital excitations of the $p = +$ kind decay relatively fast, forming the "shadow bands."

V. PARAMETER OF THE ORBITAL ORDER

In model (5) the local D_{3d} field introduces a nonequivalence of the different on-site orbital states, polarizing the t_{2g} triplet, while the antagonistic SE interaction is aimed to recover

the triplet isotropy. Therefore, a polarization of the on-site t_{2g} orbital could be a landmark of the peculiar nature of the orbital state, indicating a prevalence of one of the two mechanisms. To define this local characteristic, we rotate the quantization axes in such a way that the new $\hat{\tilde{z}}$ is directed along the cubic diagonal [111], and consider the ground-state expectation value of the component $Q^z = (\vec{l}^2 - 3l_z^2)/2$ of the t_{2g}-electron quadrupole moment as the orbital order parameter in this frame.[18] For the basis of operators (3) this quantity,

$$\langle Q^z \rangle = \langle n_{1,i} - \tfrac{1}{2}(n_{2,i} + n_{3,i}) \rangle = 1 - \tfrac{3}{2}\langle n_{2,i} + n_{3,i} \rangle, \qquad (32)$$

is expressed through the filling of the excited e'_g states. The corresponding occupation numbers are given as follows:

$$\langle n_{m,i} \rangle = -T \sum_{\vec{k}\omega} G^{mm}_{i\omega,\vec{k}} e^{+i\omega 0}, \qquad (33)$$

when employing the orbiton Green's function of Hamiltonian (12).

It is evident from Eq. (32) that the quadrupole polarization ($0 \leqslant \langle Q^z \rangle \leqslant 1$) is related to an accumulation of the orbitons in the a_{1g}-crystal level: In particular, $\langle Q^z \rangle = 1$ in the limit of the rigid orbital order. Qualitatively, $\langle Q^z \rangle$ should diminish with decreasing of $\Delta/J_{\rm SE}$, because the a_{1g} condensate $\langle n_{1,i} \rangle$ is exhausted due to the virtual e'_g excitations introduced by the spin-orbital coupling $H_{\rm int}$. In the limit of the fast orbital fluctuations ($\Delta = 0$) all the triplet levels become occupied uniformly ($\langle n_{m,i} \rangle = 1/3$ for $m = 1, 2, 3$), and thus, $\langle Q^z \rangle = 0$.

In terms of the quadrupole moment operator, interaction (4) obtains the form

$$H_{\rm LCF} = -\frac{2}{3}\Delta \sum_i Q^z_i. \qquad (34)$$

Consequently, order parameter (32) specifies the contribution $\langle H_{\rm LCF} \rangle = -2\Delta \langle Q^z \rangle/3$ of the interaction between the quadrupole polarization of the local t_{2g} electronic density and the static D_{3d} crystal field into the ground-state energy of the model (5):

$$\langle H \rangle = \langle H_{\rm LCF} \rangle + \langle H_{\rm SE} \rangle. \qquad (35)$$

The Δ dependence of the polarization, $\langle Q^z \rangle_\Delta$, evaluated from Eqs. (32) and (33) with the Green's function, calculated in the second-order perturbation theory relative $H_{\rm int}$ [taken in form (18)], is derived in Appendix B and plotted in Fig. 3. In such an approximation the orbiton–two-magnon coupling $H_{\rm int}(1)$ results in a slight decrease of $\langle Q^z \rangle$ with decreasing Δ, whereas the two-orbiton–two-magnon correction $H_{\rm int}(2)$ almost does not influence the value $\langle Q^z \rangle_\Delta$ (see the thin long-dash and thin solid line in Fig. 3, respectively).

To trace the evolution of $\langle Q^z \rangle$ upon decreasing the effective orbital gap ω_Δ, I calculate the occupation $\langle n_{2,i} + n_{3,i} \rangle$ of the e'_g states from Eq. (33) with the normal Green's function (23). Then the relation between orbital order parameter (32) and intensity of the vacuum fluctuations (D1b) is established as follows:

$$\langle Q^z \rangle = 1 - \frac{3}{2} \sum_{\substack{l=1,2 \\ p=+,-}} \left| \langle \sigma^{22}_{p,l,\vec{k}} + \sigma^{33}_{p,l,\vec{k}} \rangle_{\vec{k} \in BZ} \right|. \qquad (36)$$

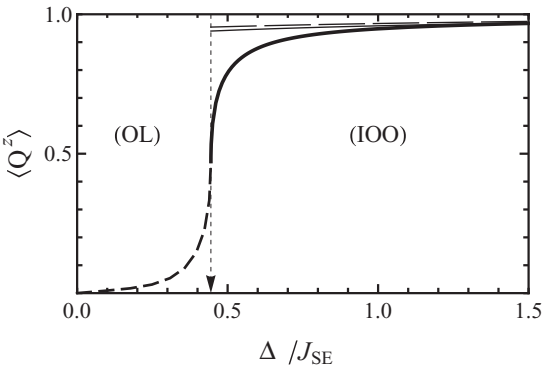

FIG. 3. Orbital order parameter as a function of $\Delta/J_{\rm SE}$ at $\langle A^{(\gamma)}_{ij} \rangle = 4/9$. The bold line is the dependence calculated from Eq. (36). The vertical arrow indicates the value $\Delta^*/J_{\rm SE} = 4/9$, where orbital gap (30) closes, providing the scale of the crossover between the regime of the IOO and OL one. The behavior of $\langle Q^z \rangle$ below $\Delta^*/J_{\rm SE}$ is schematically represented by the smooth dash curve. The thin long-dashed (thin solid) line denotes the quadrupole polarization found in the second-order perturbation theory relative $H_{\rm int}$, keeping only the three-particle contribution δQ_1 (both three- and four-particle terms δQ_1 and δQ_2) in $\langle Q^z \rangle$ [see Eq. (B5)].

The polarization $\langle Q^z \rangle$, obtained from Eq. (36) at $\langle A^{(\gamma)}_{ij} \rangle = 4/9$, is plotted versus Δ in Fig. 3 as the bold line. The progressive decrease of the order parameter with decreasing $\Delta/J_{\rm SE}$ goes hand in hand with the enhancement of the zero-point orbital oscillations (see Fig. 5 in Appendix D). The main effect on $\langle Q^z \rangle$ is provided by the quantum fluctuations related to the lowest-energy dispersion branch $\omega^-_{1,\vec{k}}$, which bring the principle contribution in the $\vec{k}$ average over the BZ in Eq. (36).

When Δ approaches Δ^* (the lower bound of the IOO state), the order parameter rapidly drops. This is related with divergence (31) of the magnitude $\sigma^{nn}_{-,1,\vec{k}}$ of the fluctuations in the region, where the gapless orbital excitations appear. Although at $\Delta = \Delta^*$ the quadrupole polarization is reduced substantially, it retains about a half of its original value: $\langle Q^z \rangle_{\Delta^*} = 0.47$. It does not vanish completely at this point, because in Eq. (36) the singularity of the function $\sigma^{22}_{-,1,\vec{k}} + \sigma^{33}_{-,1,\vec{k}}$ along the coordinate axes of the BZ is integrable in the $\vec{k}$ space.

VI. DISCUSSION

The pronounced drop of the order parameter $\langle Q^z \rangle$ at Δ^* in Fig. 3 indicates a *crossover* between two distinct *regimes* of collective orbital behavior of model (5). In one of them [the IOO ($\Delta > \Delta^*$)] the t_{2g}-triplet degeneracy is lifted by the GFOD LCF, which orders the orbitals. The contribution $\langle H_{\rm LCF} \rangle$ into ground-state energy (35) prevails over the SE term $\langle H_{\rm SE} \rangle$. In turn, the SE enforces the gapped local orbitons, mediated by the intersite virtual spin fluctuations, to cooperate, forming the extended bosonic composite modes, protected by the reduced crystal gap ω_Δ. These generalized orbital waves, developed in the IOO regime, are not the true Goldstone bosons, caused by a continuous symmetry breaking. The related vacuum oscillations admix the e'_g-doublet excitations to

the basic a_{1g} singlet state, progressively suppressing the on-site t_{2g} quadrupole moments with decreasing the ratio $\Delta/J_{\rm SE}$.

When Δ approaches the scale Δ^* and then goes below it, the substantial SE fluctuations defeat the IOO state in the antiferromagnet, breaking down the orbital gap ω_Δ. Again, the infinitely degenerate massless excitations appear in the dispersion, being an analog of the orbital frustration in the approach of Khaliullin and Maekawa[10] for the pure-SE AFM model. The orbiton-magnon SE coupling becomes strong between sites in the gapless many-particle continuum.[12] Then a formation of virtual bonds with fast spin-orbital fluctuations *à la* the intersite singlet resonances, as in Ref. 10, could be the efficient way to reduce total energy (35) of model (5) through the SE channel, when $\Delta < \Delta^*$. The enhancing orbital fluctuations further depress the quadrupole polarization $\langle Q^z\rangle$, which becomes small, and the corresponding energy $\langle H_{\rm LCF}\rangle$ diminishes below $\langle H_{\rm SE}\rangle$ in this regime. The related approximation for the resonances interacting with the distortions could be the fermionic $\chi - J$ model of the OL,[10] with its low-lying quasiparticles affected by the local D_{3d} crystal field as a perturbation. In this respect, the effect of the LCF on the OL resembles the Pauli paramagnetism, when a static magnetic field is applied to the Fermi liquid. To be more specific, the induced quadrupole polarization, remaining in the OL, could be regarded as a result of the following virtual process: The crystal field of the GFOD instantly "picks up" the orbitons from the spin-orbital resonances into the on-site states with nonzero $\langle Q^z\rangle$, and then, the localized orbitons are reabsorbed into the OL. Again, the gradual suppression of the quadrupole moments by the collective t_{2g} fluctuations (see Fig. 3) resembles the quenching of the local spin moments without a symmetry breaking in the Kondo lattice, when they are screened by quantum oscillations of the spin density of the itinerant electrons. The quantitative description of the OL regime ($\Delta < \Delta^*$) of model (6) remains for a future analysis.

The scale Δ^* of the crossover could be evaluated from Eq. (27). One obtains the lower bound estimation, $\Delta^*/J_{\rm SE} = 4/9 \approx 0.44$, with the first-order approximation (15) for the expectation value $\langle A_{ij}^{(\gamma)}\rangle$.[62] More refined treatments of a vicinity of the transition could apparently somewhat enlarge $\Delta^*(\sim 1/\langle A_{ij}^{(\gamma)}\rangle)$, because the enhancing fluctuations tend to reduce the mean field $\langle A_{ij}^{(\gamma)}\rangle$: For instance, in the OL state,[10] $\langle A_{ij}^{(\gamma)}\rangle = 0.16$ is about three times smaller than the estimation given by Eq. (15) for the classical orbital order. The other reasonings suggest that the crossover appears when the energy gains due to the orbital fluctuations ($\langle H_{\rm SE}\rangle$) and polarization ($\langle H_{\rm LCF}\rangle$) match each other. Employing the value $\langle H_{\rm SE}\rangle/J_{\rm SE} = -18\chi^2 \approx -0.93$, obtained in the OL state,[10] and assuming $\langle Q^z\rangle \approx 1/2$ at the border between these regimes, one gets the upper bound estimation $\Delta^*/J_{\rm SE} \approx 2.7$ [with χ being the parameter of the SU(4) resonance]. Thus, the condition $\Delta \approx \Delta^* \approx J_{\rm SE}$ is the likely criteria for the crossover between the OL and IOO physics of model (5), where a concurrence of the SE with the LCF term governs the orbital effects.

In the present study, theoretical model (5) omits the on-site Hund-exchange coupling of the t_{2g} electrons in the SE process $d_i^1 d_j^1 \leftrightarrow d_{i(j)}^2$. Within a properly detailed SE approach (*I*) the AFM orbital-disordered phase was found to remain robust against a weak perturbation, originating from this local coupling with the realistic constant $J_{\rm H}/U \approx 0.12$.[6,18] The Hund effect partially enhances of the nearest-neighbor spin-triplet–orbital-singlet correlations in the lattice. The related intersite orbital-singlet fluctuations cooperate with the underlying spin-orbital resonances, further reducing (by $\approx$30%) the energy $\langle H_{\rm SE}\rangle$ of the OL AFM state.[18] Estimations for suitably corrected model (5), implemented in Appendix E, conform with this physics and indicate that the corresponding effect on the scale of the crossover is small: The magnitude of Δ^* increases by $\approx$15%–20%, suggesting a slight widening of the Δ range of the orbital-fluctuation regime (OL).

Again, in the crossover region, $\Delta \approx J_{\rm SE}$, the magnitudes of $\Delta/J_{\rm SE}$ are not too far from those evaluated in genuine titanates, say in $LaTiO_3$.[46]

A technique for direct measurements of orbital states has still not been developed. They are studied only through indirect effects, introducing ambiguity in estimations for the orbital variables. In titanates with $R =$ La, Y, the static orbital polarization has been established from the splitting of the ^{47,49}Ti NMR signal due to an on-site hyperfine coupling between the nucleus spins and the electron quadrupole moments.[35,40] In these experiments the resonance was observed about frequencies $\omega_{\rm Res} \approx 20$ MHz, which are six orders of magnitude less than the orbital fluctuation rates.[63] As compared with such rapid processes, the NMR response was measured over a "wide time window"$\sim 1/\omega_{\rm Res}$, corresponding to a period of the nucleus moment precession. The nucleus resonance detects a quasistatic hyperfine field due to the mean orbital polarization.[35,40,64] Thus, an information about the orbital oscillations could be either hidden or defaced after averaging over such a wide observation window. In Refs. 10 and 65 a principle ability to resolve the SE orbital fluctuations have been proved for observations with "narrow time window,"reached in the high-frequency Raman and RIXS measurements. The corresponding effect appeared in a form of the broad peak about 0.25 eV in experiments for titanates with $R =$ La, Y.[38,39,66] The RIXS even made it possible to reveal the collective orbital dynamics; however, an uncertainty in the measured dispersion of excitations was about their magnitude, that is, too large.[39] Nevertheless, the above data definitely indicated the marked dualistic character of the t_{2g} orbitals, combining the quantum fluctuations and the static polarization in their nature.

Model (5) suggests the similar orbital bifacial states, which combines both features: quadrupole polarization and fluctuations. Response functions (23) of Hamiltonian (5) describe the states in a dependence on the frequency, covering both the low- and the high-frequency experimental "windows."In particular, a scale of the energies $2\omega_{l,\vec{k}}^-$ of the two-orbiton excitations corresponds to the location of the above-mentioned Raman peak at 235 meV.[38,67] Thus, in this respect, the model generalizes the (*I*) and (*II*) schemes.

VII. CONCLUSION

An approach has been suggested for a description of the orbital degrees of freedom of the $d^1(t_{2g})$ electrons in the perovskite Mott insulators: The model has been introduced, which unified both typical interactions, *coexisting* in the materials. One of them was the intersite SE, inducing the

fluctuations of the planar orbital. The other was the LCF due to the $GdFeO_3$-kind structure deformation, which split the t_{2g} triplet, thereby arranging the orbitals. The cubic lattice with the AFM SE bonds and on-site D_{3d} -LCF, created by the GFOD, has been chosen as a prototype of the perovskite.

The related problem of the competition between the LCF an SE interactions for the orbitals has been resolved in the limit of the vanishing Hund on-site electronic exchange coupling. A new way of organizing of these degrees of freedom has been obtained in the lattice: the *bifacial* orbital states, unifying the induced polarization and quantum fluctuations. Their dependence both on the magnitude Δ of the triplet splitting and the SE constant $J_{\rm SE}$ has been established. The transition from the classical order to the fast fluctuations has been followed. The two qualitatively different regimes, IOO ($\Delta > \Delta^*$) and OL ($\Delta < \Delta^*$), as well as the transitional region (crossover) between them have been revealed. The crossover appears when the parameters Δ and $J_{\rm SE}$ are comparable. The Hund-exchange correction to the transition scale Δ^* has been estimated to be small. In the IOO regime the orbital order is stable, and the collective oscillations resemble the waves, involving the orbital and spin variables simultaneously. The dispersion of these orbital modes, spectral characteristics of the fluctuations, and the quadrupole order parameter have been calculated in the Born approximation. When the renormalized crystal gap ω_Δ is depressed, the fluctuations overcome, and the system progressively transforms into the opposite, OL regime, possessing the remnant quadrupole polarization due to the moderate LCF.

Both preceding approaches, employing either of the interactions (LCF or SE), is found to fail in the crossover range, while they are appropriate in the corresponding regime (IOO or OL) as an initial approximation. Therein, the present investigation generalizes the previous theories, bridging the "gap" between them and identifying their validity regions. Thus, my theory provides the more comprehensive description of the orbital states, reconciling the ordering and fluctuations, while the LCF and SE schemes emphasized either of these aspects.

Again, the suggested approach is suitable to clarify the d electron physics in the family of titanates, $R\mathrm{TiO_3}$: The resembling dualism was observed in these compounds, which revealed the orbital polarization[35] and fluctuations[38,39] in the opposite frequency "windows."Apparently, the approach is also related to other t_{2g} systems, for example, vanadates, exhibiting the effects of the GFOD structure[15,41] together with the developed orbital fluctuations[42,43] as well. In $R\mathrm{VO_3}$ the issue of the interplay between these interactions demands a specific solution and will be the subject of a future work.

ACKNOWLEDGMENTS

I am very grateful to G. G. Khaliullin for many stimulating and valuable discussions, to L. R. Tagirov and A. G. Krivenko for critical reading of the manuscript, and to G. B. Teitel'baum for elucidating communications. The article has been supported by the RFBR under the Project No. 10-02-01005-a. The support and hospitality of the research group, headed by F. Mancini, at Salerno University (Italy) is appreciated as well.

APPENDIX A: FOUR-PARTICLE ORBITON-MAGNON INTERACTION $H_{\rm int}(2)$

The contribution $H_{\rm int}(2)$ to spin-orbital interaction (18) is related to the quadratic orbital operator, which reads

$$A_{ij}^{(\gamma)}(2)=\sum_{m,n=2}^{3}\left(\alpha_{x,nm}^{(\gamma)}x_{ij}^{mn}+\alpha_{y,nm}^{(\gamma)}y_{ij}^{mn}+\alpha_{z,nm}^{(\gamma)}z_{ij}^{mn}\right). \tag{A1}$$

Here the bosonic pairs are defined as follows:

$$\begin{aligned} x_{ij}^{mn} &= \psi_{m,i}^{\dagger}\psi_{n,j}+\text{H.c.},\\ y_{ij}^{mn} &= \tfrac{1}{2}[(\psi_{m,i}^{\dagger}\psi_{n,i}+\psi_{m,j}^{\dagger}\psi_{n,j})+\text{H.c.}],\\ z_{ij}^{mn} &= \psi_{m,i}^{\dagger}\psi_{n,j}^{\dagger}+\text{H.c.}, \end{aligned} \tag{A2}$$

which are denoted by the index $\zeta = x,y,z$. Also, in Eq. (A1) the numeric coefficients,

$$\begin{aligned} &\alpha_{\zeta,nm}^{(a)} = u_{\zeta}^{nm}, \quad \alpha_{\zeta,nm}^{(b)} = (-1)^{n+m}u_{\zeta}^{nm},\\ &\alpha_{\zeta,nm}^{(c)} = v_{\zeta}^{nm}, \end{aligned} \tag{A3}$$

are expressed through elements of the respective matrices

$$\begin{aligned} u_x &= \frac{1}{9}\begin{pmatrix}3 & \sqrt{3}\\ \sqrt{3} & 5\end{pmatrix}, \quad v_x = \frac{2}{9}\begin{pmatrix}3 & 0\\ 0 & 1\end{pmatrix},\\ u_y &= -\frac{1}{18}\begin{pmatrix}5 & \sqrt{3}\\ \sqrt{3} & 7\end{pmatrix}, \quad v_y = -\frac{2}{9}\begin{pmatrix}2 & 0\\ 0 & 1\end{pmatrix},\\ u_z &= -\frac{1}{18}\begin{pmatrix}-3 & \sqrt{3}\\ \sqrt{3} & -1\end{pmatrix}, \quad v_z = \frac{2}{9}\begin{pmatrix}1 & 0\\ 0 & 0\end{pmatrix}. \end{aligned} \tag{A4}$$

Having expanded the spin factor in Eq. (11) in terms of the Holstein-Primakoff bosons s_i we obtain the corresponding two-orbiton–two-magnon interaction:

$$H_{\rm int}(2) = \frac{1}{2}J_{\rm SE}\sum_{\langle ij\rangle_\gamma}\left(n_i^s+n_j^s+s_i^{\dagger}s_j^{\dagger}+s_is_j\right)A_{ij}^{(\gamma)}(2), \tag{A5}$$

where $A_{ij}^{(\gamma)}(2)$ are given by Eq. (A1), and $n_i^s = s_i^{\dagger}s_i$.

APPENDIX B: QUADRUPOLE MOMENT IN THE SECOND ORDER PERTURBATION THEORY

In this Appendix I evaluate the quadrupole polarization from Eq. (32) in the second-order perturbation theory with respect to the interaction $H_{\rm int}$, given by Eq. (18). Then the related orbiton Green's functions are calculated as follows:

$$G_{i\omega,\vec{k}}^{mn} = \frac{1}{i\omega-\Delta}+\frac{1}{(i\omega-\Delta)^2}\left[S_{i\omega,\vec{k}}^{mn}(1)+S_{i\omega,\vec{k}}^{mn}(2)\right]. \tag{B1}$$

Here the correction $S_{i\omega,\vec{k}}^{mn}(1) = S_{i\omega,\vec{k}}^{mn}$ [see Eq. (21)] is obtained with the diagram in Fig. 1(a), originating from the three-particle coupling $H_{\rm int}(1)$ [Eq. (19)]. Again, the four-particle interaction $H_{\rm int}(2)$ [Eq. (A5)] produces the next term, $S_{i\omega,\vec{k}}^{mn}(2)$, given by the diagram in Fig. 1(b) in the following form:

$$S_{i\omega,\vec{k}}^{mn}(2) = \frac{J_{\rm SE}^2L^{mn}}{-i\omega-(\Delta+2D)}+\frac{J_{\rm SE}^2R_{\vec{k}}^{mn}}{i\omega-(\Delta+2D)}, \tag{B2}$$

where

$$L^{mn} = \left(\delta_{mn} u_z^{ml} u_z^{ln} + \tfrac{1}{2} v_z^{ml} v_z^{ln}\right) p_{mln}, \tag{B3a}$$

$$\begin{aligned} R^{mn}_{\vec{k}} = {} & 2\delta_{mn}\left(u_x^{ml}u_x^{ln} + u_y^{ml}u_y^{ln}\right) + v_x^{ml}v_x^{ln} + v_y^{ml}v_y^{ln} \\ & + \left[c_{k_x} + (-1)^{m+n} c_{k_y}\right]\left(u_x^{ml}u_y^{ln} + u_y^{ml}u_x^{ln}\right) \\ & + c_{k_z}\left(v_x^{ml}v_y^{ln} + v_y^{ml}v_x^{ln}\right). \end{aligned} \tag{B3b}$$

The summation over the index $l = 2,3$ is taken in Eqs. (B3), u_ζ^{mn} ($\zeta = x,y,z$) are defined by Eqs. (A4), and Eq. (B3a) contains the factor

$$p_{mln} = (1 - \delta_{mn})(\delta_{ml} + \delta_{ln}) + \tfrac{1}{2}\delta_{mn}(3\delta_{ml} + 1). \tag{B4}$$

When orbiton functions (B1) are employed, quadrupole polarization (32) is calculated as follows:

$$\langle Q^z \rangle = 1 - \delta Q_1 - \delta Q_2, \tag{B5}$$

where the contribution

$$\delta Q_j = -\frac{3}{2} T \sum_\omega \sum_{m=2}^{3} \frac{e^{+i\omega 0}}{(i\omega - \Delta)^2} \left\langle S^{mm}_{i\omega,\vec{k}}(j) \right\rangle_{\vec{k}\in ZB} \tag{B6}$$

corresponds to the coupling $H_{\rm int}(j)$. Here the average is taken over the BZ, and $j = 1(2)$ identifies the orbiton–two-magnon (two-orbiton–two-magnon) channel. Having substituted Eqs. (21) and (B2) into (B6), we obtain the respective corrections:

$$\delta Q_1 = \frac{4}{9}\frac{J_{\rm SE}^2}{(\Delta + 2D)^2}, \qquad \delta Q_2 = \frac{3}{8}\beta\frac{J_{\rm SE}^2}{(\Delta + D)^2}, \tag{B7}$$

where

$$\beta = \sum_{m=2}^{3} L^{mm} = 13/108. \tag{B8}$$

The Δ dependencies, $\langle Q^z \rangle_\Delta$, at $\langle A_{ij}^{(\gamma)} \rangle = 4/9$, calculated from Eqs. (B5) with (B7), are plotted in Fig. 3, taking into account as only the first term δQ_1, and so both contributions δQ_1 and δQ_2 (see Sec. V for the discussion).

APPENDIX C: BORN APPROXIMATION

The orbiton propagators, being the solutions of Dyson equations (20), have the following matrix form:

$$\hat{G}_{i\omega,\vec{k}} = \frac{\hat{g}_{i\omega,\vec{k}}}{D_{i\omega,\vec{k}}}, \quad \hat{F}_{i\omega,\vec{k}} = \frac{\hat{f}_{i\omega,\vec{k}}}{D_{i\omega,\vec{k}}}. \tag{C1}$$

In particular, the function in the denominator,

$$D_{i\omega,\vec{k}} = \prod_{n=2}^{3}\left[(i\omega)^2 - \Delta^2 - 2\Delta S^{nn}_{i\omega,\vec{k}}\right] - \left(2\Delta S^{23}_{i\omega,\vec{k}}\right)^2, \tag{C2}$$

is expressed through the elements of the "mass operator" $\hat{S}_{i\omega,\vec{k}}$, and the respective matrix numerators of Eqs. (C1) are given as

$$\begin{aligned} \hat{g}_{i\omega,\vec{k}} = {} & \hat{f}_{i\omega,\vec{k}} + (i\omega + \Delta)\left\{[(i\omega)^2 - \Delta^2 - \Delta S^{+}_{i\omega,\vec{k}}]\hat{I}\right. \\ & \left. + (i\omega - \Delta) S^{23}_{i\omega,\vec{k}}\sigma_x - \Delta S^{-}_{i\omega,\vec{k}}\sigma_z\right\}, \end{aligned} \tag{C3a}$$

$$\hat{f}_{i\omega,\vec{k}} = [(i\omega)^2 - \Delta^2]\hat{S}_{i\omega,\vec{k}} - 2\Delta\hat{I}\det\hat{S}_{i\omega,\vec{k}}, \tag{C3b}$$

where $S^{\pm}_{i\omega,\vec{k}} = S^{22}_{i\omega,\vec{k}} \pm S^{33}_{i\omega,\vec{k}}$, and $\sigma_{x(z)}$ is the Pauli matrix.

The diagram in Fig. 1(a) results in the following orbiton self-energy part:

$$S^{mn}_{i\omega,\vec{k}} = \sum_{\vec{p}} g^{(m)}_{\vec{p},\vec{k}+\vec{p}}\, g^{(n)}_{\vec{p},\vec{k}+\vec{p}} \frac{2\tilde{\varepsilon}_{\vec{k},\vec{p}}}{(i\omega)^2 - \tilde{\varepsilon}^2_{\vec{k},\vec{p}}}. \tag{C4}$$

Dynamical corrections (C4) are expressed through energies $\tilde{\varepsilon}_{\vec{k},\vec{p}} = \omega_{\vec{p}} + \omega_{\vec{k}+\vec{p}}$ of corresponding pairs of the spin excitations with the dispersion $\omega_{\vec{k}} = 3J(1 - \gamma^2_{\vec{k}})^{1/2}$ and the matrix elements

$$g^{(n)}_{\vec{k},\vec{p}} = V a_n \times \left[\eta^{(n)}_{\vec{q}} N_{\vec{k},\vec{p}} + \left(\eta^{(n)}_{\vec{k}} + \eta^{(n)}_{\vec{p}}\right) M_{\vec{k},\vec{p}}\right] \tag{C5}$$

of spin-orbital interaction (19), taken in the momentum representation. Here the following definitions are employed: The interaction parameter is $V = 2\sqrt{6}J_{\rm SE}/9$, the coefficients are $a_2 = 1$, $a_3 = -2/\sqrt{3}$, the form factors of the SE bonds, $\eta^{(n)}_{\vec{k}}$, read as

$$\begin{aligned} \eta^{(2)}_{\vec{k}} &= \tfrac{1}{2}\left(c_{k_x} - c_{k_y}\right), \\ \eta^{(3)}_{\vec{k}} &= \tfrac{1}{4}\left(c_{k_x} + c_{k_y} - 2c_{k_z}\right), \end{aligned} \tag{C6}$$

and $\vec{q} = \vec{k} - \vec{p}$. Again in Eq. (C5), the terms $N_{\vec{k},\vec{p}} = u_{\vec{k}}v_{\vec{p}} + v_{\vec{k}}u_{\vec{p}}$ and $M_{\vec{k},\vec{p}} = u_{\vec{k}}u_{\vec{p}} + v_{\vec{k}}v_{\vec{p}}$ combine the Bogoliubov magnon transformation coefficients, $u_{\vec{k}} = [(s+1)/2]^{1/2}$ and $v_{\vec{k}} = -[(s-1)/2]^{1/2}\mathrm{sgn}\gamma_{\vec{k}}$, where $s = (1 - \gamma^2_{\vec{k}})^{1/2}$.

Vertex functions (C5) of the spin-orbital coupling vanish at small magnon momenta due to factors (C6), and it is the *short*-wavelength magnons which are important for the problem. In this respect, the situation is analogous to the pure-SE model.[10] Thus, in a similar way to Ref. 10, the orbital dynamics could be approached, treating the magnons in the Izing limit in the orbital self-energy, because contributions from soft-magnons are suppressed in $\vec{p}$-sum (C4) due to the matrix elements.

Then the model becomes tractable, and orbital self-energy (C4) and propagators (C1) are calculated analytically in respective form (21) and (23). In more detail, the denominator of Green's functions (23) is given by Eq. (24), and the corresponding numerators are now written as

$$g^{mn}_{i\omega,\vec{k}} = g_{i\omega,\vec{k}}\,\delta_{mn} + 4DJ^2_{\rm SE}(i\omega + \Delta)^2[(i\omega)^2 - 4D^2]c^{mn}_{\vec{k}}, \tag{C7a}$$

$$f^{mn}_{i\omega,\vec{k}} = f_{\vec{k}}\,\delta_{mn} - 4DJ^2_{\rm SE}[(i\omega)^2 - \Delta^2][(i\omega)^2 - 4D^2]c^{mn}_{\vec{k}}, \tag{C7b}$$

with $c^{mn}_{\vec{k}}$ defined by Eqs. (22). Again, in Eqs. (C7) the first terms,

$$\begin{aligned} g_{i\omega,\vec{k}} = {} & (i\omega - \Delta)(i\omega + \Delta)^2[(i\omega)^2 - 4D^2]^2 - f_{\vec{k}} \\ & - \frac{64}{27}\Delta DJ^2_{\rm SE}(i\omega + \Delta)[(i\omega)^2 - 4D^2](1 + \gamma_{\vec{k}}), \\ f_{\vec{k}} = {} & 2\left(\frac{16}{27}\right)^2 \Delta D^2 J^4_{\rm SE}\left[2\gamma_{\vec{k}} + \tfrac{1}{2}\left(3\gamma^2_{\vec{k}} - \kappa_{\vec{k}}\right) + 1\right], \end{aligned} \tag{C8}$$

combined with $\gamma_{\vec{k}}$ and $\kappa_{\vec{k}} = (c^2_{k_x} + c^2_{k_y} + c^2_{k_z})/3$ are cubically symmetric in the $\vec{k}$ space, while the second contributions to numerators (C7) violate this symmetry. Anticipating things, the extended e'_g fluctuations, deduced from functions (23),

obtain a dispersion, $\omega^{\pm}_{l,\vec{k}}$ [Eq. (25)], markedly reducing the crystal gap from the original value, Δ, to the effective one, ω_Δ [Eq. (30)].

To verify the Izing-approximation results, I have also calculated the orbital spectrum from the poles of initial Green's functions (C1), taken in their retarded form, when the magnon dynamics is treated carefully in self-energy part (C4). The low-frequency orbiton dispersion, obtained numerically, was found to indeed closely follow the dependencies $\omega^{-}_{l,\vec{k}}$; in particular, the bottom of the dispersion resembles a plateau along the same axes, $(k_x,0,0)$, $(0,k_y,0)$, and $(0,0,k_z)$. The residual coupling of the orbitons to the long-wavelength spin fluctuations stimulates a slightly more rapid decrease of the orbital gap as compare to Izing-limit value (30): For example, the gap becomes $\approx 0.85\,\omega_\Delta$, when $\Delta = 0.55$.

Such likeness of the results is explainable, because intersite interaction (19) stems from the exchange in the bonds, mainly involving the short-wavelength magnons.

APPENDIX D: SPECTRAL DENSITY OF THE ORBITAL FLUCTUATIONS

An intensity of the orbital fluctuations could be evaluated from the residues, $\rho^{mn}_{p,l,\vec{k}}$ and $\sigma^{mn}_{p,l,\vec{k}}$, in the corresponding poles, $\omega^{p}_{l,\vec{k}} \geqslant 0$ and $-\omega^{p}_{l,\vec{k}} \leqslant 0$, of the retarded normal Green's function $G^{mn(R)}_{\omega,\vec{k}}$ derived from Eq. (23). They are calculated as follows:

$$\rho^{mn}_{p,l,\vec{k}} = g^{mn}_{\omega^{p}_{l,\vec{k}},\vec{k}} \prod_{p'l'} \left(\omega^{p}_{l,\vec{k}} + \omega^{p'}_{l',\vec{k}}\right)^{-1} \dot{\prod_{p'l'}} \left(\omega^{p}_{l,\vec{k}} - \omega^{p'}_{l',\vec{k}}\right)^{-1}, \quad \text{(D1a)}$$

$$\sigma^{mn}_{p,l,\vec{k}} = g^{mn}_{-\omega^{p}_{l,\vec{k}},\vec{k}} \prod_{p'l'} \left(\omega^{p}_{l,\vec{k}} + \omega^{p'}_{l',\vec{k}}\right)^{-1} \dot{\prod_{p'l'}} \left(\omega^{p'}_{l',\vec{k}} - \omega^{p}_{l,\vec{k}}\right)^{-1}. \quad \text{(D1b)}$$

The factors, having $p' = p$ and $l' = l$ simultaneously, are omitted in the products labeled by a dot in Eqs. (D1), expressed through matrix elements (C7a) and dispersion (25).

The spectral density of the orbital wave and related zero-point mode with the frequency $\omega^{p}_{l,\vec{k}}$ are given as $\rho^{mn}_{p,l,\vec{k}}\,\delta(\omega - \omega^{p}_{l,\vec{k}})$ and $\sigma^{mn}_{p,l,\vec{k}}\,\delta(\omega + \omega^{p}_{l,\vec{k}})$, respectively, when the IOO is stable at $\Delta \geqslant \Delta^*$.

The residues $\rho^{mm}_{-,l,\vec{k}}$ ($\sigma^{mm}_{-,l,\vec{k}}$), obtained from Eqs. (D1) for the lower-energy branches $\omega^{-}_{l,\vec{k}}$, are plotted in Fig. 4 (5) against the momentum. Their marked anisotropy in the $\vec{k}$ space reflects the competition between the LCF and SE for the planar t_{2g} orbitals. The residues for the higher-energy branches ($p = +$) are skipped here, because they are by some orders of magnitude smaller than those for the lower ($p = -$) branches. See Sec. IV for a detailed discussion of the orbital fluctuations.

APPENDIX E: INFLUENCE OF THE HUND COUPLING ON THE ORBITAL STATE

The cubic-lattice Hamiltonian of the SE interaction $H^{ij}_{\rm SE}$ between the nearest-neighbor $d^1(t_{2g})$ ions is given by Eq. (1) in Ref. 18, which takes into account the Hund exchange coupling ($J_{\rm H} \ll U$) in the on-site virtual $d^2(t_{2g})$ states. Its relevant spin-orbital contribution $H_{\rm SE}$, coming into operation in orbital

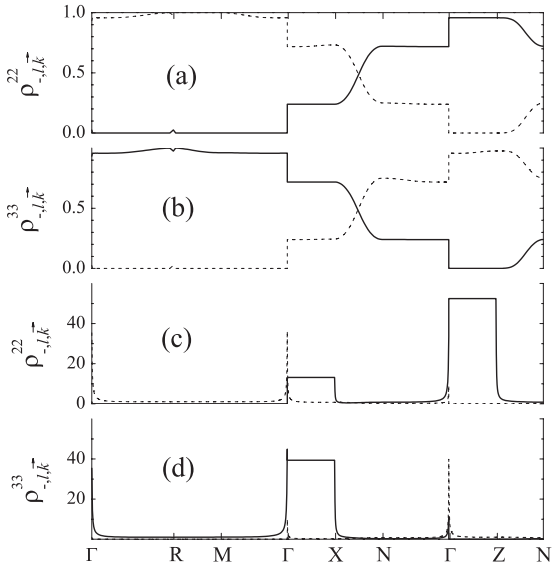

FIG. 4. Momentum dependence of the residue $\rho^{mm}_{-,l,\vec{k}}$ [see Eq. (D1a)] in the pole $\omega^{-}_{l,\vec{k}}$ of the retarded orbiton Green's function $G^{mm(R)}_{\omega,\vec{k}}$ ($m = 2,3$) at $\langle A^{(\gamma)}_{ij}\rangle = 4/9$. The solid (dashed) line corresponds to the index $l = 1$ (2). The data in panels (a) and (b) are calculated with the triplet splitting $\Delta = J_{\rm SE}$, when the orbital gap is open; again, those in panels (c) and (d) are obtained with the parameter $\Delta = \Delta^* + 10^{-5} J_{\rm SE}$, which approaches the scale Δ^* when the gap disappears. The path goes through the same points as in Fig. 2 including $Z = (0,0,\pi)$.

model (5), retains the form of KK SE term (1), where the spin exchange integral is modified as follows: $J_{\rm SE} A^{(\gamma)}_{ij} \to J_{\rm SE} \tilde{A}^{(\gamma)}_{ij}$. The adjusted orbital operator,

$$\tilde{A}^{(\gamma)}_{ij} = \tfrac{1}{2}(r_1 + r_2) A^{(\gamma)}_{ij} - \tfrac{1}{3}(r_2 - r_3) B^{(\gamma)}_{ij} - \tfrac{1}{4}(r_1 - r_2)(n_i + n_j)^{(\gamma)}, \quad \text{(E1)}$$

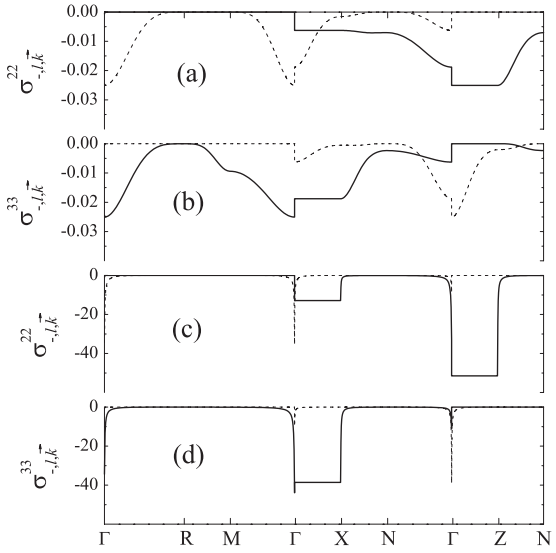

FIG. 5. Momentum dependence of the residue $\sigma^{mm}_{-,l,\vec{k}}$ [see Eq. (D1b)] in the pole $-\omega^{-}_{l,\vec{k}}$ of the retarded function $G^{mm(R)}_{\omega,\vec{k}}$ ($m = 2,3$). The respective notations and parameter values are the same as in Fig. 4.

provides the model with a dependence on the Hund-coupling strength $\eta = J_H/U$ via the coefficients $r_1 = 1/(1-3\eta)$, $r_2 = 1/(1-\eta)$, and $r_3 = 1/(1+2\eta)$. In Eq. (E1) the term $A_{ij}^{(\gamma)}$ stands for previous operator (2), while $B_{ij}^{(\gamma)}$ and $n_i^{(\gamma)}$ are written as

$$\begin{aligned} B_{ij}^{(c)} &= n_{i,a}n_{j,a} + n_{i,b}n_{j,b} + a_i^\dagger b_i a_j^\dagger b_j + b_i^\dagger a_i b_j^\dagger a_j, \\ n_i^{(c)} &= n_{i,a} + n_{i,a} \end{aligned} \tag{E2}$$

for the bonds along the direction c. Expressions for the bonds a and b are obtained by replacing of the orbiton pairs (a,b) by (b,c) and (c,a) in Eqs. (E2), respectively.

We employ the approach developed in Sec. II C. Then the expansion of orbital operator (E1) into the mean field $\langle \tilde{A}_{ij}^{(\gamma)} \rangle$ and fluctuation $\delta\tilde{A}_{ij}^{(\gamma)}$, corresponding to the e'_g excitations about the a_{1g} IOO state due to the SE interaction, is calculated as

$$\tilde{A}_{ij}^{(\gamma)} = \alpha_{0,\eta}\langle A_{ij}^{(\gamma)} \rangle + \alpha_{1,\eta} A_{ij}^{(\gamma)}(1). \tag{E3}$$

Here the initial expectation value $\langle A_{ij}^{(\gamma)} \rangle$ and linear operator $A_{ij}^{(\gamma)}(1)$ are given by Eqs. (15) and (16), respectively, while their "Hund corrections" have the following form:

$$\alpha_{0,\eta} = \frac{1-\frac{5}{2}\eta}{1-2\eta}, \quad \alpha_{1,\eta} = \frac{1-\frac{7}{4}\eta}{1-2\eta}. \tag{E4}$$

In the IOO regime of the antiferromagnet, the model for the orbital dynamics is reduced to Hamiltonian (12), where the parameters of the terms H_{sp} and H_{int} (respectively the magnon bandwidth $D = 3J$ and orbiton-magnon coupling constant J_{SE}) become renormalized as follows:

$$\begin{aligned} H_{sp} &: D \to D_\eta = \alpha_{0,\eta} D, \\ H_{int} &: J_{SE} \to J_\eta = \alpha_{1,\eta} J_{SE}. \end{aligned} \tag{E5}$$

Then the orbital Green's functions, excitation spectrum, and polarization $\langle Q^z \rangle$ are directly deduced from foregoing Eqs. (23), (25), and (36), respectively, after substitution of the corresponding parameters in conformity with rule (E5). The lengthy explicit expressions are skipped here.

The Hund corrections to the orbital states of model (5) are found to be small: A representative value[18] of η about 0.12 results in $\alpha_{0,\eta} \approx 0.92$ and $\alpha_{1,\eta} \approx 1.04$; that is, orbital operator (E3) rescales by 5%–10%. This estimation quantifies deviations of the intersite exchange integral, orbiton dispersion, and orbital order parameter from the initial ones, when the Hund coupling is included.

The gap of the orbiton dispersion is obtained to vanish along $\vec{k} = (0,0,k_z)$ and equivalent directions in the BZ, when the trigonal splitting Δ approaches the modified lower bond of the IOO regime Δ_η^*. The scale is found as

$$\Delta_\eta^* = \frac{\alpha_{1,\eta}^2}{\alpha_{0,\eta}} \Delta^*, \tag{E6}$$

where its initial evaluation $\Delta^* (= \frac{4}{9} J_{SE} \approx 0.44 J_{SE})$ is provided by Eq. (27) and indicated by the arrow in Fig. 3. With realistic[18] η, relation (E6) yields $\Delta_\eta^*/\Delta^* \approx 1.17$; that is, $\Delta_\eta^* \approx 0.52 J_{SE}$. This implies a slight increase (by ≈15%–20%) of the lower-bond estimation of the scale Δ^* of the crossover from the IOO toward the orbital-disordered regime, when the Hund electronic correlations are included in model (5).

Again, in the pure-SE scheme the ground-state energy E_0 of the AFM state with the fast orbital fluctuations is calculated per lattice bond as follows: $E_0/J_{SE} \approx 6\chi^2 \approx -0.31$,[10] and $E_0(\eta)/J_{SE} \approx -0.33(r_1+r_2)/2$,[18] when the Hund interaction is neglected and included, respectively. This suggests that the upper-bond estimation of the crossover scale (discussed in Sec. VI) also tends to increase with increasing J_H when $\eta \ll 1$, because $\Delta_\eta^*/\Delta^* \approx E_0(\eta)/E_0 \approx (r_1+r_2)/2 > 1$. Namely, $\Delta_\eta^*/\Delta^* \approx 1.35$ when $\eta = 0.12$, implying the rough upper-bond evaluation $\Delta_\eta^* \approx 3.6 J_{SE}$.

The physics behind the related tendency toward a small widening of the Δ range of the orbital-disordered regime in the phase diagram could be the following: Violating the spin-SU(2) symmetry, the AFM arrangement partially unbalances the spin-orbital configurations of the SU(4) resonances, introducing intersite short-range orbital-triplet correlations into the OL ground state.[10] In turn, the competing small perturbation of the SE bonds due to the Hund-effect promotes the nearest-neighbor spin-triplet–orbital-singlet correlations, thus stimulating intersite orbital-singlet fluctuations in the OL.[6] Adopted into the collective OL-like resonances, these virtual short-range singlets could provide more SE-energy gain from the orbital fluctuations, being the plausible origin of the aforesaid reduction of E_0 in the AFM orbital-disordered state.[18] It should be mentioned here that the channel of the orbital-singlet fluctuations dominates in the case of $d^2(t_{2g})$ systems (vanadates), where the Hund interaction becomes substantial.[6,16,43]

*s.a.krivenko@mail.ru

[1] M. Imada, A. Fujimori, and Y. Tokura, Rev. Mod. Phys. **70**, 1039 (1998).

[2] Y. Tokura and N. Nagaosa, Science **288**, 462 (2000); Y. Tokura, Phys. Today **56**, 50 (2003).

[3] K. I. Kugel and D. I. Khomskii, Usp. Fiz. Nauk **136**, 621 (1982); Sov. Phys. Usp. **25**, 231 (1982)].

[4] S. Maekawa, T. Tohyama, S. E. Barnes, S. Ishihara, W. Koshibae, and G. Khaliullin, *Physics of Transition Metal Oxides*, Springer Series in Solid State Sciences, Vol. 144 (Springer-Verlag, Heidelberg, 2004).

[5] M. Mochizuki and M. Imada, New J. Phys. **6**, 154 (2004).

[6] G. Khaliullin, Prog. Theor. Phys. Suppl. **160**, 155 (2005).

[7] L. F. Feiner and A. M. Oleś, Phys. Rev. B **59**, 3295 (1999); S. Okamoto, S. Ishihara, and S. Maekawa, *ibid.* **65**, 144403 (2002).

[8] T. Mizokawa, D. I. Khomskii, and G. A. Sawatzky, Phys. Rev. B **60**, 7309 (1999).

[9] S. Ishihara, T. Hatakeyama, and S. Maekawa, Phys. Rev. B **65**, 064442 (2002).

[10] G. Khaliullin and S. Maekawa, Phys. Rev. Lett. **85**, 3950 (2000).

[11] G. Khaliullin, Phys. Rev. B **64**, 212405 (2001).

[12] K. Kikoin, O. Entin-Wohlman, V. Fleurov, and A. Aharony, Phys. Rev. B **67**, 214418 (2003).

[13] A. M. Oleś, P. Horsch, L. F. Feiner, and G. Khaliullin, Phys. Rev. Lett. **96**, 147205 (2006).

[14] A. M. Oleś, P. Horsch, and G. Khaliullin, Phys. Status Solidi B **244**, 2378 (2007).
[15] P. Horsch, A. M. Oleś, L. F. Feiner, and G. Khaliullin, Phys. Rev. Lett. **100**, 167205 (2008).
[16] G. Khaliullin, P. Horsch, and A. M. Oleś, Phys. Rev. Lett. **86**, 3879 (2001); P. Horsch, G. Khaliullin, and A. M. Oleś, *ibid*. **91**, 257203 (2003); A. M. Oleś, P. Horsch, and G. Khaliullin, Phys. Rev. B **75**, 184434 (2007).
[17] G. Khaliullin and S. Okamoto, Phys. Rev. Lett. **89**, 167201 (2002).
[18] G. Khaliullin and S. Okamoto, Phys. Rev. B **68**, 205109 (2003).
[19] M. Mochizuki and M. Imada, Phys. Rev. Lett. **91**, 167203 (2003).
[20] M. Mochizuki and M. Imada, J. Phys. Soc. Jpn. **73**, 1833 (2004).
[21] M. Cwik, T. Lorenz, J. Baier, R. Müller, G. André, F. Bourée, F. Lichtenberg, A. Freimuth, R. Schmitz, E. Müller-Hartmann, and M. Braden, Phys. Rev. B **68**, 060401 (2003).
[22] E. Pavarini, S. Biermann, A. Poteryaev, A. I. Lichtenstein, A. Georges, and O. K. Andersen, Phys. Rev. Lett. **92**, 176403 (2004).
[23] R. M. Eremina, M. V. Eremin, V. V. Iglamov, J. Hemberger, H.-A. Krug von Nidda, F. Lichtenberg, and A. Loidl, Phys. Rev. B **70**, 224428 (2004).
[24] R. Schmitz, O. Entin-Wohlman, A. Aharony, A. B. Harris, and E. Müller-Hartmann, Phys. Rev. B **71**, 144412 (2005).
[25] R. Schmitz, O. Entin-Wohlman, A. Aharony, A. B. Harris, and E. Müller-Hartmann, Phys. Rev. B **71**, 214438 (2005).
[26] E. Pavarini, A. Yamasaki, J. Nuss, and O. K. Andersen, New J. Phys. **7**, 188 (2005).
[27] I. V. Solovyev, Phys. Rev. B **69**, 134403 (2004).
[28] S. V. Streltsov, A. S. Mylnikova, A. O. Shorikov, Z. V. Pchelkina, D. I. Khomskii, and V. I. Anisimov, Phys. Rev. B **71**, 245114 (2005).
[29] I. V. Solovyev, Phys. Rev. B **74**, 054412 (2006).
[30] M. Mochizuki and M. Imada, J. Phys. Soc. Jpn. **70**, 2872 (2001).
[31] V. V. Iglamov and M. V. Eremin, Phys. Solid State **49**, 229 (2007).
[32] A. A. Mozhegorov, A. E. Nikiforov, A. V. Larin, A. V. Efremov, L. E. Gontchar, and P. A. Agzamova, Phys. Solid State **50**, 1795 (2008); A. A. Mozhegorov, A. V. Larin, A. E. Nikiforov, L. E. Gontchar, and A. V. Efremov, Phys. Rev. B **79**, 054418 (2009).
[33] B. Keimer, D. Casa, A. Ivanov, J. W. Lynn, M. v. Zimmermann, J. P. Hill, D. Gibbs, Y. Taguchi, and Y. Tokura, Phys. Rev. Lett. **85**, 3946 (2000).
[34] D. A. MacLean, H. N. Ng, and J. E. Greedan, J. Solid State Chem. **30**, 35 (1979); M. Eitel and J. E. Greedan, J. Less-Common Met. **116**, 95 (1986).
[35] T. Kiyama and M. Itoh, Phys. Rev. Lett. **91**, 167202 (2003).
[36] M. W. Haverkort, Z. Hu, A. Tanaka, G. Ghiringhelli, H. Roth, M. Cwik, T. Lorenz, C. Schüßler-Langeheine, S. V. Streltsov, A. S. Mylnikova, V. I. Anisimov, C. de Nadai, N. B. Brookes, H. H. Hsieh, H.-J. Lin, C. T. Chen, T. Mizokawa, Y. Taguchi, Y. Tokura, D. I. Khomskii, and L. H. Tjeng, Phys. Rev. Lett. **94**, 056401 (2005).
[37] M. Reedyk, D. A. Crandles, M. Cardona, J. D. Garrett, and J. E. Greedan, Phys. Rev. B **55**, 1442 (1997).
[38] C. Ulrich, A. Gössling, M. Grüninger, M. Guennou, H. Roth, M. Cwik, T. Lorenz, G. Khaliullin, and B. Keimer, Phys. Rev. Lett. **97**, 157401 (2006).
[39] C. Ulrich, L. J. P. Ament, G. Ghiringhelli, L. Braicovich, M. M. Sala, N. Pezzotta, T. Schmitt, G. Khaliullin, J. van den Brink, H. Roth, T. Lorenz, and B. Keimer, Phys. Rev. Lett. **103**, 107205 (2009).
[40] T. Kiyama, H. Saitoh, M. Itoh, K. Komada, H. Ichikawa, and J. Akimitsu, J. Phys. Soc. Jpn. **74**, 1123 (2005).
[41] S. Miyasaka, Y. Okimoto, M. Iwama, and Y. Tokura, Phys. Rev. B **68**, 100406(R) (2003); S. Miyasaka, J. Fujioka, M. Iwama, Y. Okimoto, and Y. Tokura, *ibid*. **73**, 224436 (2006).
[42] C. Ulrich, G. Khaliullin, J. Sirker, M. Reehuis, M. Ohl, S. Miyasaka, Y. Tokura, and B. Keimer, Phys. Rev. Lett. **91**, 257202 (2003).
[43] S. Miyasaka, S. Onoda, Y. Okimoto, J. Fujioka, M. Iwama, N. Nagaosa, and Y. Tokura, Phys. Rev. Lett. **94**, 076405 (2005).
[44] P. W. Anderson, Phys. Rev. **115**, 2 (1959).
[45] K. I. Kugel and D. I. Khomskii, Sov. Phys. Solid State **17**, 285 (1975).
[46] Regarding a relation between energy scales of the competing interactions in the t_{2g} orbital Mott insulators, then, for instance, in $LaTiO_3$ the evaluation $J_{SE} \approx 100$ meV of the parameter of the SE interaction in Ref. 10 does not differ too much from the magnitude of the crystal gap Δ, though estimations of the last one are somewhat scattered. For example, density functional-based *ab initio* calculations result in Δ, varied from 37 to 54 meV (see Refs. 27 and 29) to 140 meV (Ref. 22). Again, cluster LCAO computations in Ref. 32 brought 180 meV, while the gap, obtained with different LCF models (Refs. 21, 24, and 31), was about 200 to 240 meV. Also, in Ref. 36 x-ray and spin-polarized photoemission measurements, interpreted using the local density approximation, yielded 120 to 300 meV for the t_{2g} triplet splitting.
[47] A. B. Harris, T. Yildirim, A. Aharony, O. Entin-Wohlman, and I. Ya. Korenblit, Phys. Rev. Lett. **91**, 087206 (2003).
[48] N. D. Mermin and H. Wagner, Phys. Rev. Lett. **17**, 1133 (1966).
[49] For introduction to the order-from-disorder phenomena in frustrated systems, see, for example, A. M. Tsvelik, *Quantum Field Theory in Condensed Matter Physics* (Cambridge University Press, Cambridge, 1995), Chap. 17; and *Frustrated Spin Systems*, edited by H. T. Diep (World Scientific, Singapore, 2005).
[50] G. Khaliullin and V. Oudovenko, Phys. Rev. B **56**, R14243 (1997); G. Khaliullin and R. Kilian, J. Phys. Condens. Matter **11**, 9757 (1999).
[51] The e_g-orbital frustration of the KK SE model remains an intricate problem; in the cubic lattice its exact solution is unknown. The chainlike orbital order represents the likely ground state, when the Hund-exchange is neglected (see Ref. 50). The phase diagram of the generalized model was deduced to contain transitions into various alternative spin-orbital states, including entangled ones; see the articles L. F. Feiner, A. M. Oleś, and J. Zaanen, Phys. Rev. Lett. **78**, 2799 (1997); J. Phys. Condens. Matter **10**, L555 (1998); for the resent progress in this research see W. Brzezicki and A. M. Oleś, Phys. Rev. B **83**, 214408 (2011).
[52] Y. Q. Li, M. Ma, D. N. Shi, and F. C. Zhang, Phys. Rev. Lett. **81**, 3527 (1998).
[53] Y. Q. Li, M. Ma, D. N. Shi, and F. C. Zhang, Phys. Rev. B **60**, 12781 (1999).
[54] B. Frischmuth, F. Mila, and M. Troyer, Phys. Rev. Lett. **82**, 835 (1999).
[55] F. Mila, B. Frischmuth, A. Deppeler, and M. Troyer, Phys. Rev. Lett. **82**, 3697 (1999).
[56] S.-Q. Shen, Phys. Rev. B **64**, 132411 (2001).

[57] P. W. Anderson, Mater. Res. Bull. **8**, 153 (1973); Science **235**, 1196 (1987).

[58] SE interaction (1) is taken under the assumption of vanishing strength $J_{\rm H}$ of the Hund exchange. The AFM coupling is expected between the spins due to the SE within t_{2g} states, when $J_{\rm H}/U$ is small (Refs. 18–20). A detailed description of the interplay between the LCF and SE in a dependence on parameter $J_{\rm H}$ represents a challenge for future studies, particularly in a regime of the spin-orbital entanglement.

[59] For more details about the relative role of the three- and four-particle spin-orbital interactions $H_{\rm int}(1)$ and $H_{\rm int}(2)$ for the orbital state, see the discussion in Sec. V also.

[60] It has been similarly argued in Ref. 10, that the Izing-magnon approximation is appropriate to resolve the spin-orbital coupling problem even in the pure-SE model, which corresponds to the case of the gapless orbitons, $\Delta = 0$, in my study.

[61] For the lowest-energy orbital excitations $\omega^{-}_{1,\vec{k}}$ the functions $\rho^{mm}_{-,1,\vec{k}}$ and $\sigma^{mm}_{-,1,\vec{k}}$ possess divergence (31) along the three axes $\alpha = x$, y, z in the reciprocal space, when $m = 2$; for $m = 3$ it arises only for $\alpha = x$, y, while along z the residues are zero. For the next branch $\omega^{-}_{2,\vec{k}}$ of the dispersion the functions $\rho^{mm}_{-,2,\vec{k}}$ and $\sigma^{mm}_{-,2,\vec{k}}$ obtain only an isolated singularity in the origin Γ, which is not important.

[62] A minor coupling of the orbitons to the long-wavelength magnons, still retained by SE vertex (C5), additionally stimulates the ground-state fluctuations via dynamical corrections (C4) to Green's functions (C1). Then evaluations within the Born approximation beyond the Izing-magnon limit provide that the transition from the IOO to the gapless OL-regime appears a bit in advance, about $\Delta \approx \Delta^{*} \approx 0.51 J_{\rm SE}$, as compared to the above-mentioned lower-bond estimation $\Delta^{*} = 0.44 J_{\rm SE}$.

[63] An estimation of a typical rate of the quantum orbital fluctuations could be obtained from the energies $\omega^{-}_{l,\vec{k}}$ of the lower orbiton band: The corresponding scale is about 10^{7} MHz when $\Delta \approx J_{\rm SE}$.

[64] C. P. Slichter, *Principles of Magnetic Resonance* (Springer-Verlag, New York, 1980), Chap. 5.

[65] L. J. P. Ament and G. Khaliullin, Phys. Rev. B **81**, 125118 (2010).

[66] C. Ulrich, G. Ghiringhelli, A. Piazzalunga, L. Braicovich, N. B. Brookes, H. Roth, T. Lorenz, and B. Keimer, Phys. Rev. B **77**, 113102 (2008).

[67] For a discussion of Raman-active orbital effects, see, e.g., R. Rückamp, E. Benckiser, M. W. Haverkort, H. Roth, T. Lorenz, A. Freimuth, L. Jongen, A. Möller, G. Meyer, P. Reutler, B. Büchner, A. Revcolevschi, S.-W. Cheong, C. Sekar, G. Krabbes, and M. Grüninger, New J. Phys. **7**, 144 (2005).